A NON-AGGREGATIVE, THERMALLY STABLE GLUCOSE SENSOR FOR CONTINUOUS GLUCOSE MONITORING

A Dissertation

by

ANDREA KRISTINE LOCKE

Submitted to the Office of Graduate and Professional Studies of
Texas A&M University
in partial fulfillment of the requirements for the degree of

DOCTOR OF PHILOSOPHY

Chair of Committee,	Gerard L. Coté
Committee Members,	Melissa A. Grunlan
	Francios P. Gabbai
	Fred J.Clubb
Head of Department,	Anthony Guiseppi-Elie

August 2016

Major Subject: Biomedical Engineering

ABSTRACT

Diabetes mellitus is a disease that affects the regulation of a person's blood glucose levels. Fully implantable continuous glucose monitoring (CGM) has the potential to improve diabetes management by improving patient compliance and more importantly, providing patients with a more detailed trend of their glucose level on a daily basis. One such approach in the development of a CGM device is the use of the lectin Concanavalin A (ConA) in a competitive glucose binding assay. The current set back to these ConA based assay has to do with its stability, and sensitivity. Furthermore, current CGM devices face longevity issues due to the nature of the implant and attack from the immune system.

Therefore, the overall goal of the project is to develop a fully implantable, minimally invasive CGM device that would overcome issues pertaining to longevity, stability and sensitivity. Towards this goal, the current work aimed to first develop a non-aggregative thermally stable glucose sensing assay. First, ConA's thermal stability at body temperature (37 ^{o}C) was evaluated and based on the resulting instability, ConA was modified with poly (ethylene glycol) chains to improve its thermal stability at 37 ^{o}C. Results showed that the presence of these PEG chains improved ConA's thermal stability without significantly hindering its ability to bind to a competing ligand and sense changes in glucose concentrations within the physiologically relevant range.

Next, this worked characterized the sensitivity and FRET efficiency of the newly modified ConA based assay, paired with the recently introduced monovalent competing

ligand, mannotetraose. These characteristics was compared to current traditional ConA/dextran based glucose sensing assay. It was determined that across the desired glucose concentration range of 0 to 600 mg/dL, the new PEGylated ConA/mannotetraose based assay had improved sensitivity and FRET efficiency when compared to a PEGylated ConA/dextran based assay.

Finally, this work aimed to encapsulate the modified assay within the proposed biocompatible membrane, PNIPAAm, and evaluate its ability to sense changes in external glucose concentration. To accomplish this, different encapsulation techniques such as calcium carbonate microspheres, alginate microspheres and layer by layer (LbL) deposition on PNIPAAm copolymer AMPS (AMPS-PNIPAAm) hydrogels were investigated to achieve minimal leaching without significantly impacting the glucose sensing of the assay within a hollow rod shaped membrane. The work also investigated the modification of the assay to increase the size of the smaller assay component as an alternative means to try and retain the assay within the biocompatible membrane. The deposition of LbL on the inner wall of the AMPS-PNIPAAm rods proved to be more efficient with an approximate 50% change in FRET signal for changes in glucose concentration ranging from 0 to 600 mg/dL and a mean absolute relative difference (MARD) of ~10%.

DEDICATION

In memory of my grandmother Hadie Swift and my aunt Barbara Young.

ACKNOWLEDGEMENTS

I would like to thank Dr. Gerard Coté, my committee chair, for his guidance and support throughout the course of my graduate degree. I could not have asked for a better advisor. Thank you for this opportunity which allowed be to grow not only as a researcher but also as a research mentor.

Thanks to my committee members, Dr. Melissa Grunlan, Dr. Fred Clubb, and Dr. Francois Gabbai, for their counsel and support.

Thanks to the Engineering Academic and Student Affairs office for the student worker opportunity which kick started my journey towards furthering my education.

I am grateful for my friends in the Optical BioSensing Lab, BioSyM lab and the Biomedical Engineering Department as a whole, thank you for making my graduate study such a great experience and for uplifting me during difficult times.

Most importantly, I would like to thank my family and Joy Monroe for their unconditional love, support, encouragement and supply of food.

NOMENCLATURE

AMPS	2-Acrylamido-2-Methylpropane Sulfonic Acid
APTS	8-Aminopyrene-1,3,6-Trisulfonic Acid
CGM	Continuous Glucose Monitoring
CL	Competing Ligand
ConA	Concanavalin A
DLS	Dynamic Light Scattering
DN	Double Network
FA	Fluorescence Anisotropy
FITC	Fluorescein Isothiocyanate
FRET	Forster Resonance Energy Transfer
LbL	Layer-by-Layer
mPEG	Methoxyl-Poly (Ethylene Glycol)
MT	Mannotetraose
MARD	Mean Absolute Relative Difference
MW	Molecular Weight
PAH^+	Poly (Allylamine)
$PDADMAC^+$	Poly (Diallyldimethylammonium Chloride)
PEG	Poly (Ethylene Glycol)
PNIPAAm	Poly (*N*-isopropylacrylamide)
PSS^-	Poly (Sodium 4-Styrenesulfonate)

RT	Room Temperature
TRITC	Tetramethylrhodamine Isothiocyanate
wt%	Weight Percent

TABLE OF CONTENTS

Page

LIST OF FIGURES

Page

LIST OF TABLES

Page

CHAPTER I

INTRODUCTION AND BACKGROUND REVIEW*

Diabetes

The carbohydrate molecule, glucose is an important source of nutrient within the body. Therefore, its physiological concentration level needs to be maintained in order for most biological processes to function properly. However, for approximately 29 million people within the United States (U.S.) and over an estimated 300 million worldwide, their bodies are unable to properly regulate and maintain its glucose level within the normal range of 80 mg/dL to 130 mg/dL.[1, 2] This is known as the disease Diabetes mellitus and it is largely related to problems surrounding the production and regulation of the insulin hormone.

There are three classes or types of this disease, Type I (Juvenile Diabetes), Type II, and Gestational diabetes. Type I is due to the body's inefficiency to produce insulin because of destruction to the beta cells of the pancreas.[3] It is typically diagnosed during childhood and affects an estimated five percent of the U.S. population. Type II, is the most common form of Diabetes, where the body does not produce enough insulin or does not use it properly.[3] Gestational diabetes is linked to pregnancy where it is assumed that due to the rise in hormonal levels, typically around 24 weeks, there is a disruption of

* Part of this chapter is reprinted with permission from A.K. Locke, B. M. Cummins, A. A. Abraham and G. L. Coté. " PEGylation of Concanavalin A to Improve Its Stability for an In Vivo Glucose Sensing Assay," *Analytical Chemistry* **2014**, 85(11), 5397-5404. Copyright 2014 American Chemical Society; and from A.K. Locke, B. M. Cummins, and G. L. Coté. "High Affinity Mannotetraose as an Alternative to Dextran in ConA Based Fluorescent Affinity Glucose Assay Due to Improved FRET Efficiency," *ACS Sensors* **2016**, 1 (5), 584-590. Copyright 2016 American Chemical Society.

the mother's use of insulin.[3] In each of these cases, if normal physiological glucose concentration is not maintained the outcome can be very detrimental to the patient's health. The advent of low physiological glucose concentration (hypoglycemia) may result in coma and/or death, while high glucose concentrations (hyperglycemia) can cause long term, secondary complications. These complications include kidney failure, gangrene leading to amputations, heart disease and nerve damage. These secondary risks have a tremendous impact on the quality of life of patients and the cost of their healthcare expenditure.[4] Therefore, there is a need for patients to tightly monitor their glucose level in order to treat any deviations through insulin injections, diet, and/or exercise.

History of Glucose Monitoring

The first generation of devices designed to monitor physiological glucose were qualitative urine tests. In 1941, Bayer introduced Clinitest®, an alkaline copper sulphate reagent tablet which changed color from green to orange with increasing concentration of glucose.[5] In the 1950s and 1960s, glucose test tapes/strips such as "Tes-Tape", "Dipstix" and "Diastix" were introduced. These test strips are able to indirectly detect glucose via an enzymatic reaction involving glucose oxidase which is immobilized on tip of these strips. If glucose is present, the strip also changed color corresponding to an estimated glucose concentration.

Although these devices are low cost and painless the major drawbacks are their failure to detect hypoglycemia and difficulty in interpreting the colorimetric changes.

Therefore, the second generation devices were developed to be more accurate and provide a quantitative methodology for self-monitoring of the glucose level within the blood. These devices include the well-known "finger-prick" test using a glucometer. The Ames Reflectance Meter was the first glucometer developed in the 1970s by Anton Clemens.[6] This device utilized the enzymatic reagent blood test strip, Dextrostix which required a small droplet of blood that was washed away after one minute. The glucose within the blood, in the presence of oxygen, reacted with the immobilized GOx. One of the by-product, hydrogen peroxide, then reacted with a reducing dye on the test strip which changed color. The reflectance meter then shined a light on the test strip and the reflected light is analyzed to provide a quantitative value correlating to glucose concentration. The darker the color change, due to higher glucose concentration, the less light reflected back. However it was reported that the device became unstable and inaccurate above 180 mg/dL.[7] Since this development, there have been numerous improvement on the design including portability, use of electrochemical sensor to improve sensitivity and accuracy, elimination of the blood removal step, reduction in the required volume of blood and faster testing time.[8]

To date, this "finger prick" test is the most common way that patients self-monitor their glucose level. It is recommended that measurements be taken at least five times per day. However, this method which requires the repetitive puncture of the skin results in low patient compliance. Furthermore, because this test only provides a few time points of the patient's glucose level, they may be unaware of times when they are approaching or are already experiencing critical levels. This has lead researchers and

several medical device companies to investigate new ways in developing next generation devices categorized as “continuous glucose monitoring” device in order to overcome the current problem associated with the finger-prick method.

Third generation devices are geared towards continuous glucose monitoring (CGM), non-invasively or minimally invasive, which have the potential to provide patients the necessary information for them to be able to better manage their glucose level. These devices involve using different optical techniques such as Fluorescence spectroscopy, Near Infrared spectroscopy, Raman spectroscopy, and Polarimetry.[9-11]

Currently, there are only a few commercially available CGM devices approved by the Food and Drugs Administration (FDA). These devices include: (1) Dexcom™ G4 Platinum (7 days lifetime), (2) Dexcom™ SEVEN Plus (7 days lifetime), and (3) MiniMed Guardian® (3 days lifetime) by Medtronic. Each device display and record data in five min intervals and have the ability to alert patients when they are approaching hypoglycemic or hyperglycemic levels. However, their need for frequent calibration via the “finger prick” test, weekly replacement due to limited lifetimes, as well as their transdermal sensor component which cause skin irritation limits the wide impact that these devices can have in the monitoring of the disease. Thus, there is still a need to develop new sensors that do not require frequent calibration and can be fully implanted or integrated non-invasively to improve on the longevity of the devices.

Herein, this work focused on the design of a fully implantable fluorescence based CGM devices because of its potential to achieve higher sensitivity to glucose over the other techniques.

Fluorescence Based Continuous Glucose Monitoring

When a molecule absorbs energy its electron is excited to a higher energy level, upon return to its ground state it emits a photon and this phenomenon is known as fluorescence. Generally, the emitted light occurs at a longer wavelength than the excitation light. This emission can be isolated using filters and measured using a photo-detector. Fluorescence based sensors are advantageous because of they are highly sensitive and have known to be very favorable to molecular based detection due to its high signal to noise ratio.[12] As a result, fluorescence has been greatly used as the basis for glucose sensing. Fluorescence based glucose sensors generally involve systems that utilizes energy transfer, the monitoring of enzymatic consumption or intrinsic fluorescence and measures either the fluorescence intensity or lifetime of the fluorophore. Three most common fluorescence based glucose sensors: (1) glucose oxidase based assays, (2) boronic acid derivatives, and (3) Concanavalin A competitive assay are discussed in this section.

Glucose Oxidase Based Sensors

Enzymes are commonly used as sensor components to indirectly track different biological analyte because of their high specificity. In terms of glucose sensing, Glucose oxidase (GOx) is the most common enzyme used. Because this is an indirect reaction resulting in the production of gluconic acid and hydrogen peroxide as by-products, glucose can indirectly be monitored in three different ways: (1) by measuring the changes in pH due to gluconic acid formation, (2) measuring the hydrogen peroxide produced, and (3) measuring the oxygen consumed. Although specific, enzymatic based

sensing relies on a stable, controllable environment. This becomes problematic *in vivo* affecting the sensitivity and stability of the sensors.

Boronic Acid Derivative Sensors

Boronic acid covalently binds to 1,2-or 1,3-diols and results in a cyclic ester bond.[13] This binding is reversible and has led to the use of boronic acid as a sensor. Furthermore, boronic acid contains a six carbon ring and as a result exhibits fluorescence properties. However, the excitation and emission wavelengths are short, 200 to 350 nm excitation and 400 to 500 nm emission range which limit its physiological usage. Yoon and Czarnik first proposed an anthyrlboronic acid based sensor for carbohydrate sensing. Anthyrlboronic acid when in water can fluorescently emit around 416 nm upon excitation.[14] When the pH of its environment becomes more basic, the fluorescence intensity decreased and Yoon *et al* suggested that this change maybe due to Chelation Enhanced Quenching. When carbohydrates such as fructose were introduced, it was noted that the intensity decreased as the pK_a of the system was approximately 8.8.[14] It is important to note that this fluorescence sensor showed a higher sensitivity to fructose than glucose but it was the first reported study which showed that boronic acid derivatives may be used for the sensing of carbohydrates. Since this study many researchers have studied the use of boronic acid derivatives as potential glucose sensors.

Each of these fluorescence based sensors have shown potential for use as a CGM device. Herein, this work focus on ConA based CGM devices since it does not consume

glucose, it's stable within physiological pH and it can easily be labelled with a fluorophore that can be interrogated *in vivo*.

Concanavalin A Based Sensors

Concanavalin A (Con A) is a lectin which binds to carbohydrates and is derived from jack bean. Under certain pH conditions it takes on either a dimeric (pH <7) or tetrameric (pH>7) conformation.[15, 16] In order to bind to glucose, manganese ions (Mn^{2+}) and calcium ions (Ca^{2+}) needs to be present to activate the binding site. However, because ConA is not selective to which carbohydrate it binds to, the binding association of the carbohydrate in relation to ConA is important. For example, ConA has a higher binding affinity to α-D-glucose than β-D-glucose. Therefore ConA based sensors typically involves a competitive displacement of a molecule in the presence of another which has a higher binding affinity to ConA. ConA based glucose sensors are favorable because unlike the enzymatic sensors, they do not require the consumption of glucose to provide information about the concentration of glucose that is present. However, the toxicity of the lectin has been questioned but recent studies have shown that if ConA does leach out of the sensor, the concentration is not significant to cause harm.[17] Herein, the three most common ConA based sensors are discussed in this section.

Con A and Dextran

The most researched competitive assay sensor is comprised on ConA and fluorescently labeled dextran. Dextran is a polysaccharide that has a binding affinity to ConA that varies based on its molecular weight (MW). In 1982, Schultz, Mansouri and

Goldstein pioneered a technique for developing implantable sensors for glucose using ConA and fluorescein-labeled dextran (FITC dextran).[18] This approach was based on the competitive displacement of dextran, from ConA binding sites, in the presence of glucose and the measurement of the unbound FITC-dextran to determine an approximate concentration of glucose present. Since this introduction, many researchers have tried to improve the sensitivity of ConA/dextran based sensors.

Furthermore, there are now several companies developing CGM devices based on this technology to achieve improved sensitivity, accuracy, and working lifetime. Also, more recently research conducted by Ballerstadt *et al.* have led to the development of a fiber coupled CGM device, currently under license with BioTex Inc. as a second generation Fluorescence Affinity Sensor (FAS).[19] *In vivo* human studies recently conducted on this device showed a mean absolute relative error of 13% over a period of 4 hours.[20] In addition, Muller *et al.* in 2013 introduced another fiber coupled CGM device called FiberSense.[21] This device showed improved MARD percentage over a longer period of time (14 days).[21] Both FiberSense and the second-generation FAS are transdermal CGM devices which have the possible disadvantage of irritation at the implant site due to continuous movement of the transdermal optical fiber. The PreciSense A/S device proposed by Nielsen *et al.* and recently acquired by Medtronic has the potential to overcome this disadvantage due to it being a fully implanted degradable microsensor. In a preclinical *in vivo* study, this microsensor displayed in a MARD of 11.4% over a period of 70 hours.[22] All three devices can be categorized as fluorescent affinity sensors and are based on a competitive binding assay.

Modified Con A and thiolated β-cyclodextrins (β-SH-CDs)

Quantum dots (QDs) have been used to create glucose sensors. QDs have unique optical properties such as minimal photobleaching, narrow emission band, and broad excitation band that make them good candidates to be used as sensor components. A FRET-based glucose sensor composed of Concanavalin A (ConA)-conjugated CdTe QDs and thiolated β-cyclodextrins (β-SH-CDs)-modified AuNPs was investigated.[23] Briefly, when the glucose concentration is low, β-CDs attach to the receptor protein ConA and the fluorescence caused by the QDs is quenched by the gold nanoparticles (AuNPs); however, as the glucose concentration increases, glucose molecules displace β-CDs and bind to ConA, thus allowing the fluorescence emitted by the QDs to be detected.

The advantages of this approach are its sensitivity and selectivity. However, the toxicity of QDs and the low working range of this sensor hinder its advancement for *in vivo* use.

Con A and Glycodendrimer

Recently, an alternative approach to the Con A/dextran assays was proposed. This new method utilizes polyamidoamine (PAMAM) dendrimers as the competing ligand instead of dextran. Results showed the detection of glucose (0 to 300 mg/dL) within 5 minutes.[24] Like dextran, dendrimer is a multivalent glycoconjugate and therefore have multiple binding sites for ConA molecules to interact with. However, dendrimer has more available mannose residues than dextran, thus increasing its binding affinity to ConA an improving its sensitivity in detecting glucose.[25] However, more recent work published by

Cummins in 2013, suggested that although these multivalent assays result in higher binding affinity, one main challenge is the lifespan and reversibility over longer periods of time due to these aggregates. The results suggested that assays with multivalent competing ligands had high sensitivity initially but over time the fluorescence intensity became unstable as a result of long term aggregation.[26] Therefore, in 2014, Cummins *et al* introduced a new competing ligand, mannotetraose, that is based on monovalent binding with ConA to overcome aggregation and reversibility issues without affecting the high binding affinity required to be sensitive to changes in physiological glucose concentration.[27]

Current Work on ConA/Mannotetraose Based Glucose Sensing Assay

Recently, mannotetraose was introduced as a potential alternative competing ligand with improved sensitivity and reversibility due to its non-aggregative nature when bound to ConA. Mannotetraose consist of three mannose residues that can fully bind to an individual binding site on ConA.[28] The nature of its binding produces the high binding affinity that is required for glucose sensing, when bound to ConA without the production of aggregates.

Herein, this work explored the development of a FRET assay based on this ConA/Mannotetraose pair. It examined its binding affinity under FRET conditions, and its FRET efficiency and sensitivity to changes in physiologically relevant glucose concentration compared to traditionally used competing ligand, dextran. Finally, this work aimed to encapsulate this assay within a thermo-responsive biocompatible

membrane and it evaluated the assay's glucose sensing capabilities from within the membrane.

CHAPTER II

PEGYLATION OF CONA TO IMPROVE THERMAL STABILITY[*]

Introduction

ConA, a lectin extracted from the jack bean, is a tetramer at physiological pH (7.4) comprised of four identical monomeric subunits (MW~25 kDa).[29, 30] Each monomer contains an independent carbohydrate binding site, for which glucose and mannose monosaccharide can bind.[16] It has been shown that ConA has the ability to reversibly bind to glucose with an affinity of ~400 M^{-1}.[31] This affinity allows the capability for ConA to track physiologically relevant glucose concentrations. Therefore, ConA is an attractive receptor to be used in a next generation non-enzymatic based glucose sensor.

The first noted ConA-based competitive binding assay for glucose sensing was developed by Schultz *et al.* and employed 70 kDa fluorescein-isothiocyanate dextran (FITC-dextran) as the competing ligand.[32] This scheme used a semi-permeable membrane to contain the sensing assay and allowed glucose to equilibrate with the device's external environment. Changing glucose concentrations within the membrane changed the equilibrium binding of assay components, which was transduced into a fluorescent signal that could be measured. Since this introduction, many different variations of the sensing assay have been designed and studied using the same scheme due to its tremendous potential for use in CGM devices.[33-38] Certain assay variations have immobilized ConA to

[*] Part of this chapter is reprinted with permission from A.K. Locke, B. M. Cummins, A. A. Abraham and G. L. Coté. " PEGylation of Concanavalin A to Improve Its Stability for an In Vivo Glucose Sensing Assay," *Analytical Chemistry* **2014**, 85(11), 5397-5404. Copyright 2014 American Chemical Society.

a solid-phase (microdialysis membranes, beads, etc.) while leaving the competing ligand in free solution.[39] This approach has been shown to track glucose concentrations in the body for up to 16 days.[20] Other variations have left both assay components in free solution. Practically, this approach allows the sensor to be developed modularly, where the assay can be developed without requiring the semi-permeable membrane. In addition, this approach can potentially minimize the equilibration time to changes glucose concentrations. However, the solution based approach has shown problems with stability which is a major obstacle in the advancement of the technology.[26]

This instability has partly been due to the specific sugar-dependent, aggregation seen in assays that pair traditional high-affinity competing ligands (e.g. dextran, glycosylated dendrimer, etc.) with ConA in free solution.[40, 41] Since ConA is a tetramer, it presents multiple binding sites that can aggregate with these multivalent competing ligands over time. The resulting lattice-type aggregate eventually precipitates out of solution and requires a significantly high concentration of glucose to break it apart. This type of instability has recently been addressed by the introduction of a new type of fluorescent competing ligand. This ligand avoids this specific aggregation by presenting a single high affinity moiety for ConA to bind. As a result, the ligand does not present additional residues for ConA to bind once it is already bound, allowing for the assay to remain stable in free solution.

Another aspect of the original assay's instability is associated with ConA's thermal denaturation at physiological temperatures. Since ConA is a protein, it is prone to un-folding, aggregation, and degradation.[42, 43] At elevated temperatures, the associated energy

can increase the likelihood that the protein unfolds. This unfolding can expose the hydrophobic residues, typically found in the interior of the protein, to the solvent. These residues can then interact with neighboring exposed hydrophobic groups leading to aggregation. This aggregation is believed to be irreversible and diminishes the solubility and activity of the protein.[34, 44] Vetri *et al.* have reported that ConA undergoes this denaturation-induced aggregation at ~40 ^{o}C.[45] Changes in ConA's activity due to aggregation can significantly impact the glucose response of the assay by changing the concentration of active binding sites for which glucose can bind. Therefore, to maximize the *in vivo* lifetime of a ConA-based glucose assay, it is desirable to minimize the rate of ConA's thermal denaturation at physiologically relevant temperatures. The immobilization of ConA to the solid-phase presumably maintains the assay's stability by either stabilizing ConA and/or preventing unfolded ConA from aggregating with itself.

In addition to this thermal denaturation, ConA has a tendency to adhere to positively charged surfaces. This electrostatic interaction is due to ConA's overall negative charge under physiological conditions with isoelectric point (pI), defined as the pH at which a particular molecule carries no net electrical charge, for ConA is a pI~5.[46] This adhesion of ConA to surfaces or molecules can change the concentration and the activity of the receptor in solution. This becomes important when considering encapsulation of the assay for the purpose of *in vivo* implantation. Layer-by-layer (LbL) microcapsules are attractive semi-permeable candidates that can be tuned to effectively encapsulate the assay while allowing for the rapid equilibration of smaller analytes with its exterior environment (e.g. glucose). However, proteins have shown the tendency to

electrostatically attach to the capsule's inner charged surface.[47] If ConA behaves in a similar manner, the functionality of the assays would be affected as the availability of active receptors within the capsules may decrease. Thus, if LbL micro-capsules are to be used, it would be preferable for ConA to avoid undergoing electrostatic interactions with the capsule.[48]

PEGylation is the process by which PEG chains are covalently attached to various molecules and surfaces to improve their stability, solubility, and biocompatibility.[49, 50] The enhanced stability and solubility of a molecule (e.g. protein) via PEG chains is believed to be a result of a hydration barrier created by the grafted hydrophilic chains.[51] In addition, the rapid mobility of the chains provides a steric hindrance effect that may aid in the reduction of particle-particle interaction depending on the chain length.[52] These characteristics of PEG are believed to aid in the reduction of protein aggregation and precipitation. Groups such as Rajan *et al.*, Rodriguez-Martinez *et al.* and Veronese *et al.* have shown evidence of this with the attachment of different molecular weight PEG chains to protein molecules such as α-chymotrypsin and a hematopoietic cytokines.[53-55] Furthermore, Wu *et al.* have showed an additional advantage of the chains in the role of masking surface charges to minimize non-specific electrostatic binding of proteins or cells to their imaging contrast agent.[56]

These characteristics have allowed for PEGylation to be used to improve drug delivery systems, reduce protein adhesion, and increase molecular solubility in free solution. In terms of ConA, Kim and Park have shown that the conjugation of PEG chains to ConA increased its solubility at room temperature (22 ^{o}C) for the purpose of designing

a hydrogel comprised of immobilized ConA for insulin delivery.[57, 58] Herein, we investigate the use of PEGylation to minimize the aforementioned non-specific interactions of ConA to improve the associated stability of the solution-based glucose monitoring approach in a physiologically relevant environment. We show that PEGylation decreases the rate of ConA aggregation with itself at body temperature without significantly affecting the binding affinity to the fluorescent competing ligand and its ability to track physiological glucose concentrations. We also observe that PEGylation reduces the electrostatic interactions between the lectin and positively charged surfaces which may prove to be useful for microencapsulation of the assay for *in vivo* glucose sensing.

PEGylation of ConA and Characterization

ConA was PEGylated with 5 kDa mPEG-NHS (SC), a primary amine reactive polymer that contains a succinimidyl carbonate linker. Briefly, ConA was dissolved in sodium bicarbonate buffer (10 mg/mL). The solution's peak absorbance at ~280 nm was measured using a Hitachi U-4100 UV-Vis-NIR spectrophotometer (Hitachi High Technologies American Inc., U.S.) to determine the concentration of the solution using an extinction coefficient of 118,560 $M^{-1}cm^{-1}$ based on the $E_{1\%}$ of 11.4 and MW of ~104 kDa.[59] A highly-concentrated aliquot of MaM was added to the ConA solution for a final MaM concentration of 1.9 mg/mL in an attempt to protect the activity of the binding sites of ConA during the reaction. Next, mPEG-NHS (SC) was added at a molar ratio of 16:1 to the ConA monomer. At 22 ^{o}C, this solution was mixed on a rotating wheel for 6

h and then allowed to continue reacting for an additional 18 h without mixing. The solution was subsequently separated into two dialysis tubes (MWCO 20 kDa). The first tube was dialyzed against sodium bicarbonate buffer for PEGylation characterization with fluorescamine, while the other was dialyzed against TRIS buffer for all other experiments. Following dialysis, absorption measurements were again performed to determine the final PEGylated ConA concentrations, using the same molar extinction coefficient as unmodified ConA.

The average degree of PEGylation was estimated using fluorescamine, as it is a useful tool to track the concentration of primary amines within a solution.[60] Fluorescamine becomes fluorescent after reacting with primary amines, and changes in fluorescence intensity can be descriptive of the makeup of the solution. This was used to compare identical concentrations of unmodified and PEGylated ConA to determine their relative concentrations of primary amines. This difference is related to the approximate number of mPEG chains grafted per ConA monomer.

Briefly, a range of concentrations of unmodified ConA and PEGylated ConA (0 to 2.5 μM) were prepared in sodium bicarbonate buffer (1.5 mL). Then, 500 μL of fluorescamine (0.3 mg/mL in acetone) was added to each solution and mixed well. Subsequently, 100 μL of each solution was added to a standard black 96-well microplate. After 5 minutes, the fluorescence intensity of each solution was measured using a TECAN Infinite 200 PRO microplate reader (Tecan Group Ltd, Männedorf, Switzerland) at λ_{ex} = 390 nm and λ_{em} = 475 nm. These fluorescence intensities were plotted against the corresponding ConA concentrations, and the linear regression was

performed to obtain the slopes, $m_{mPEGConA}$ and m_{ConA}. These slopes were used in Equation 1 to estimate the average degree of PEGylation (DP), similar to Wen *et al*.[61]

$$DP = \left(1 - \frac{m_{mPEGConA}}{m_{ConA}}\right) * 13$$

Equation 1.

This equation was utilized under the assumptions that fluorescamine could originally interact with each of the primary amines on unmodified ConA and that it could interact with each of the primary amines that remained on PEGylated ConA. Therefore, the differences in the fluorescence intensities are assumed to be solely due to the decrease in the primary amine concentration resulting from the conjugated PEG chains.

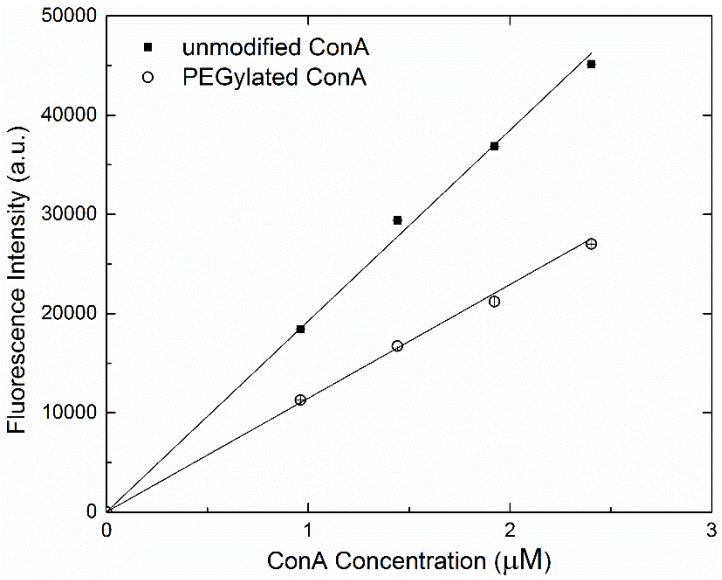

Figure 1. Fluorescence intensity of fluorescamine in the presence of PEGylated and native ConA to determine the degree of PEGlyation.

Each ConA monomer contains thirteen primary amines that can potentially be PEGylated (12 lysine residues and the N–terminus).[58] Figure 1 shows that fluorescamine's fluorescence intensity was consistently lower in solutions of PEGylated ConA than it was for unmodified ConA at the same concentration. This indicates that the presence of the mPEG chains decreased the interaction between fluorescamine and the primary amines on the PEGylated ConA. Equation 1 estimates an average of ~5 mPEG chains grafted per ConA monomer. Assuming a Poisson distribution, this degree of PEGylation would mean that 99.9% of ConA tetramers have 8 or more mPEG chains per tetramer. While the average number of mPEG chains grafted per ConA could be lower than the estimated value from Equation 1, the PEGylated ConA is expected to be sufficiently modified for the purpose of this study.

Aggregation Study via Dynamic Light Scattering Study to Determine Thermal Stability

The thermal denaturation of unmodified and PEGylated ConA in free solution was tracked by monitoring the aggregation in a physiologically relevant buffer with dynamic light scattering (DLS). In sealed disposable polystyrene cuvettes (1 cm path-length), solutions of unmodified and PEGylated ConA (10 μM each) were prepared in triplicate in TRIS buffer. The cuvettes were incubated at 37 ^{o}C. Over the course of 30 days, measurements were taken at seven different time points (Day: 0, 1, 2, 4, 9, 16, and 30) with re-suspension of the particles via aspiration before each measurement. A Malvern Nano Zetasizer (Malvern Instruments Ltd., Worcestershire, UK) was used to

measure the average particle diameter (Z-average) as well as the poly-dispersity index (PDI) of the particles within each solution.

Per Figure 2, the average particle size in the unmodified ConA solution displayed an initial (i.e. Day 0) diameter of 8 $\pm$ 0.03 nm, consistent with previous reports for the hydrodynamic diameter of unmodified tetrameric ConA.[62] The average particle size in the PEGylated ConA solution displayed a higher initial diameter of 30 $\pm$ 0.22 nm (Figure 2), due to the increase in the aforementioned hydration barrier associated with multiple mPEG chains.

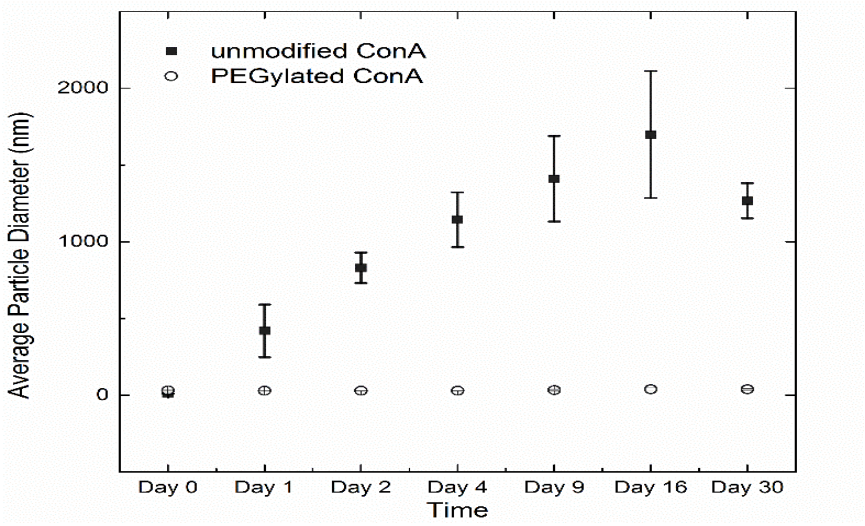

Figure 2. The Z-average particle size of native, unmodified ConA versus PEGylated ConA to determine how each respond to temperature at 37 ^{o}C over the course of 30 days.

After 24 hours, the average diameter of particles in the unmodified ConA solution increased to over 400 nm. After 30 day at 37 ^{o}C, the average diameter of particles in the solution of unmodified ConA increased to ~1.8 μm (Figure 2), indicating

aggregation of the ConA molecules. The slight decrease in particle size for unmodified ConA be-tween Day 16 and Day 30 is believed to be due to the precipitation of the larger aggregates during the measurements. Overall, this type of aggregation clearly indicates that unmodified ConA is thermally unstable in this environment.

In contrast, Figure 2 shows that the average particle size in the PEGylated ConA solution remained relatively constant at ~30-38 nm over 30 days at 37 ^{o}C. This indicates that PEGylated ConA displays negligible thermally-induced aggregation and suggests that ConA's thermal stability has indeed been improved via this degree of PEGylation. The slight increase in standard error of the average size of PEGylated ConA could be due to the small percentage of ConA molecules that displays either low levels of PEGylation or no PEGylation at all. Without sufficient PEGylation this population is expected to display properties similar to that of unmodified ConA. Strategies could potentially be employed to remove this small percentage prior to the use of PEGylated ConA in a sensor.

The poly-dispersity of the particle sizes within a solution can also be used to describe that solution. For instance, aggregation is expected to produce a large distribution of particle sizes, which would display a high level of poly-dispersity. For the DLS measurements reported here, the poly-dispersity index (PDI) indicates the level of poly-dispersity and ranges from 0 (low dispersity) to 1 (completely disperse).

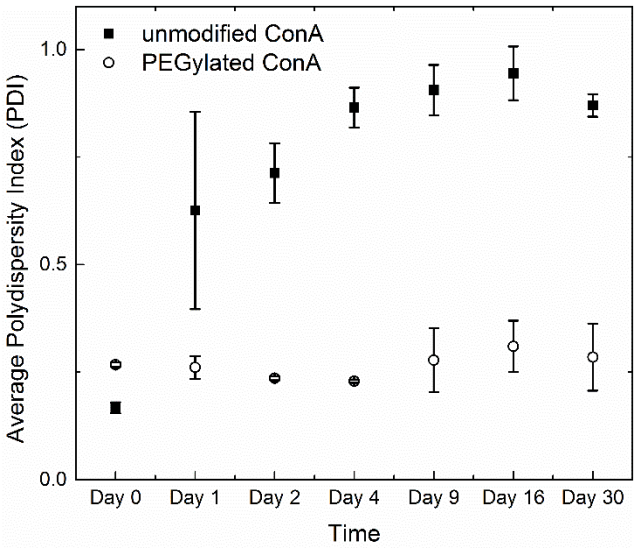

Figure 3. The average PDI of native, unmodified ConA compared to PEGylated ConA after exposure to 37 ºC for 30 days.

Figure 3 shows the comparison of time-dependent PDI of the solutions for unmodified and PEGylated ConA at 37 ºC. Initially, the PDI of the PEGylated ConA is slightly higher than the unmodified ConA. This is presumably due to the range of degrees of PEGylation that is to be expected with a Poisson distribution. However, over the course of the 30 days, of this experiment, the PDI of the unmodified ConA solution increased from 0.2 to 0.87 implying that the solutions of unmodified ConA became increasingly heterogeneous as the formation of aggregates increased (Figure 3). In comparison, Figure 3 shows that PEGylated ConA remained relatively homogeneous in solution over the same time period. This result confirms what was observed in Figure 2; the average particle size of PEGylated ConA remains relatively constant and does not aggregate. These characteristics suggest that this degree of PEGylation improves the stability of ConA at physiological conditions. It is important to note that this improved

stability could be due to an inhibition of the aggregation of unfolded ConA via steric hindrance, an improved conformational stability of ConA, or a combination thereof.

Binding Affinity Study Using Fluorescence Anisotropy

The binding affinity of unmodified and PEGylated ConA to the rationally-designed fluorescent competing ligand, APTS-MT, was evaluated using fluorescence anisotropy. In the wells of a standard black 96-well microplate, solutions were prepared with a fixed concentration of APTS-MT (100 nM) and a range of concentrations of either unmodified or PEGylated ConA (4 nM to 10 μM). Solutions were prepared in TRIS buffer, and each well had a final volume of 100 μL. The appropriate controls (TRIS buffer & 100 nM APTS-MT) were also added to separate micro-plate wells for baseline correction purposes. Time was then given for all solutions to reach equilibrium (~10 min) at 22 ^{o}C, and a TECAN Infinite F200 microplate reader fitted with polarizers was used to measure the steady-state fluorescence anisotropy of each solution (λ_{ex} = 483 nm; λ_{em} = 540 nm). The affinity was determined by plotting the average anisotropy as function of the tetrameric ConA concentration on a logarithmic scale and fitting the data with a Boltzmann curve.

To determine the stability of this binding in a physiologically relevant environment, the stock solution of PEGylated ConA was then stored at 37 ^{o}C for 30 days. Portions of this stock solution were withdrawn at various time points during this period (Days: 1, 2, 4, 9, 16, and 30) and tested via fluorescence anisotropy in the same manner.

While PEGylation does increase the stability of ConA, the PEGylated protein must maintain its binding capability to be functional in a competitive binding assay. The degree to which ConA's binding is affected by PEGylation is likely to be dependent on the chain length and the number of chains grafted. However, for a given degree of PEGylation, it is expected to have a greater effect on the binding of the competing ligand than that of glucose due to relative size. Therefore, ConA's binding to the fluorescent competing ligand (APTS-MT) of the competitive binding assay was investigated. For PEGylated ConA to be used in a competitive binding assay and optimally track physiological glucose concentrations, an affinity of 10^5 to 10^7 M^{-1} to the competing ligand is required.[28] Similar binding studies would need to be performed if a different competing ligand or degree of PEGylation were to be used. If this competing ligand was a traditional competing ligand, additional experiments should be performed to determine whether sugar-dependent aggregation is occurring. It is possible that the PEGylation of ConA could avoid the aggregation with such ligands through steric hindrance effects. Herein, the binding affinity (K_a) of APTS-MT to unmodified and PEGylated ConA was evaluated using fluorescence anisotropy. Fluorescence anisotropy is a useful tool that can provide information about protein-ligand interactions. Briefly, polarized light is used to selectively excite a portion of the fluorescent ligand within solution. The average rotational diffusion of the molecules at equilibrium can be tracked with the polarization of the fluorescence. This fluorescence polarization/anisotropy increases as the binding of the fluorescent ligand to the desired protein increases.[63] The parallel and perpendicular

components of the fluorescent emission can be measured, and the fluorescence anisotropy can be calculated with Equation 2.[64]

$$r = \frac{I_{vv} - (I_{vh} * G)}{I_{vv} + (2 * I_{vh} * G)}$$

Equation 2.

In this equation, *r* is the anisotropy, *G* is the correction factor due to the instrument's sensitivity or biased to one polarizer over the other, and I_{vv} and I_{vh} are the vertically and horizontally polarized fluorescence intensities, respectively. The dissociation constant (K_d) was determined from a plot of the anisotropy as a function of varying mPEG-ConA ($\log_{10}$ [mPEG-ConA ConA]) concentration using a Boltzmann curve fit (Equation 3).

$$r = F_0 + \frac{(F_\infty - F_0)}{1 + \exp\left(\frac{K_d - x}{slope}\right)}$$

Equation 3.

The association constants (K_a) for unmodified and PEGylated ConA were ~5.7 $\pm$ 0.37 x 10^6 M^{-1} and ~5.4 $\pm$ 0.37 x 10^6 M^{-1}, respectively. Therefore, PEGylation did not significantly affect the binding affinity of ConA to the competing ligand. Moreover, PEGylated ConA's affinity falls within the range necessary for this assay to be optimized across physiological glucose concentrations.

In addition, the capability of PEGylated ConA to maintain its binding affinity after incubation at 37 ^{o}C was evaluated. Since anisotropy is sensitive to scatter, measurements of unmodified ConA were not possible due to the large aggregate formation similar to those observed during the thermal studies.

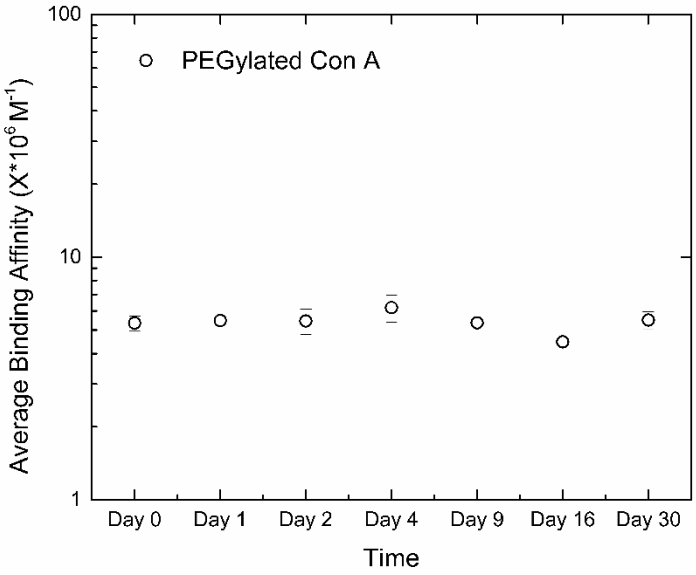

Figure 4. Binding affinity of PEGylated ConA to the competing ligand demonstrating its stability over 30 days.

Figure 4 indicates that the binding affinity of PEGylated ConA to the competing ligand remained stable at ~5.4 $\pm$ 0.5 x 10^6 M^{-1} over 30 days. The slight fluctuations in affinity may be related to pipette error during mixing and sample transfer from the cuvette to the microplate. This result, along with its thermal stability in free solution, suggests that the activity of ConA can be maintained via PEGylation which may allow for long term functionality of a ConA-based sensor. Furthermore, because ConA's binding is due to its folded structure, the long term binding stability suggests that the

protein maintains its functional conformation over time. Therefore, we expect that PEGylation is most likely enhancing ConA's conformational stability in addition to any steric-hindrance effects that it also imparts.

Non-Specific Adsorption Study

Light scatter can be used to investigate the interaction of macromolecules in free solution, including those containing proteins. For example, Park *et al.* have used this method to study the electrostatic interaction between different biological proteins (i.e. BSA, RNase and lyzozymes) and poly-electrolytes (i.e. PSS, PVS, etc.) via turbidity measurements at 420 nm.[65] This turbidity is related to the amount of aggregation within the various samples and is indicative of the specific and/or nonspecific binding between molecules.

In a similar manner, the electrostatic interactions of PAH^+ (a common polyelectrolyte used in LbL) with un-modified and PEGylated ConA was measured in this study. ConA absorbs ultraviolet light with a peak at ~280 nm, and absorbs a negligible amount of light above ~320 nm. Therefore, any extinction of the incident light higher than 320 nm is assumed to be scattered light that is associated with aggregate formation within the solution.

In separate centrifuge tubes, each of the following solutions was prepared in triplicate in TRIS buffer at 22 ^oC: PAH^+ with ConA, PAH^+ with PEGylated ConA, ConA, PEGylated ConA, and PAH^+. Each individual component in each solution was prepared at 10 μM for comparison. Immediately after preparation, 100 μL of each

sample was extracted and added to a standard UV-Vis 96-well microplate. The turbidity of each solution was then measured at 400 nm using a TECAN Infinite 200 PRO® microplate reader. These measurements were also performed at 30 min, 1 h, 24 h, and 48 h.

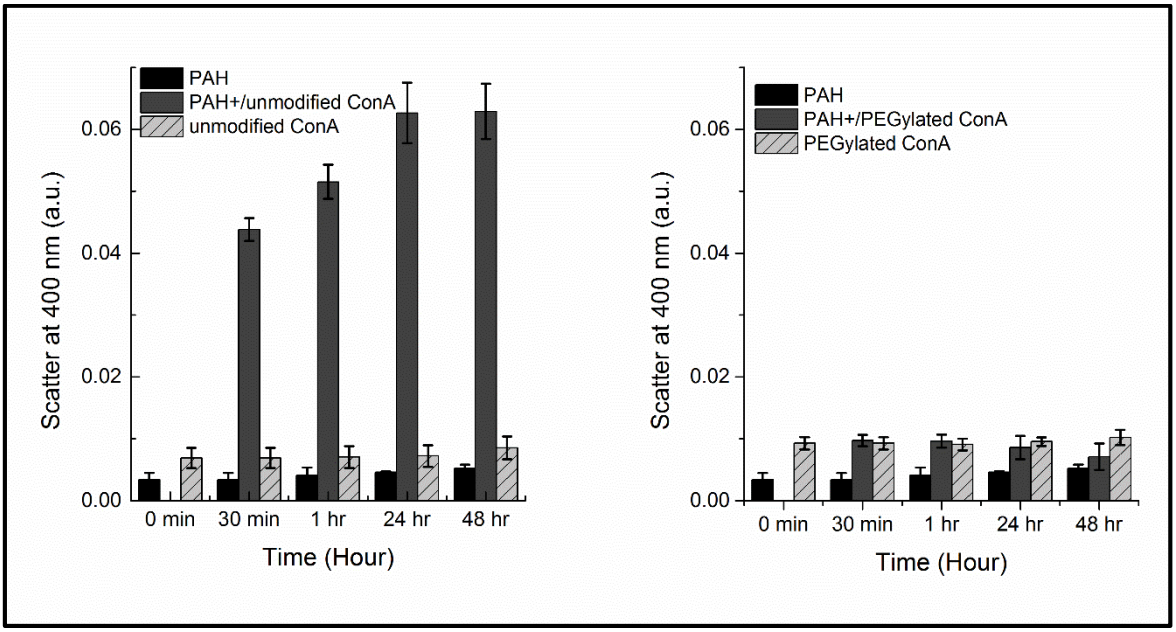

Figure 5. Scattering effect due to electrostatic interaction between native, unmodified ConA (left) and PEGylated ConA (right) with PAH^+.

The electrostatic-induced aggregation between the negatively charged unmodified ConA and the positively charged PAH^+ is observed with the increase in scatter in comparison to its control, unmodified ConA without PAH^+ (Figure 6). Moreover, the unmodified ConA/PAH^+ aggregates were observed as white particulates within the solution (Figure 7). In contrast, PEGylated ConA's interaction with PAH^+ showed relatively no change in scattering, indicating no aggregate formation. This may

be due to the masking of the charges on ConA by the mPEG chains, and thereby preventing ConA adhesion to PAH^+. To validate this data, separate solutions of ConA, PEGylated ConA, and PAH^+ were used as controls. During the same time period there were no changes in scatter of these controls. This establishes that the increase in scatter was a direct result of the interaction between unmodified ConA and PAH^+. Therefore, PEGylation proved useful in the minimization of electrostatic-induced aggregation of ConA. This is desirable when aiming to encapsulate the ConA based assay within a carrier (e.g. layer-by-layer microcapsules) as it may allow the assay to remain free in solution and thus, maintain its full activity.

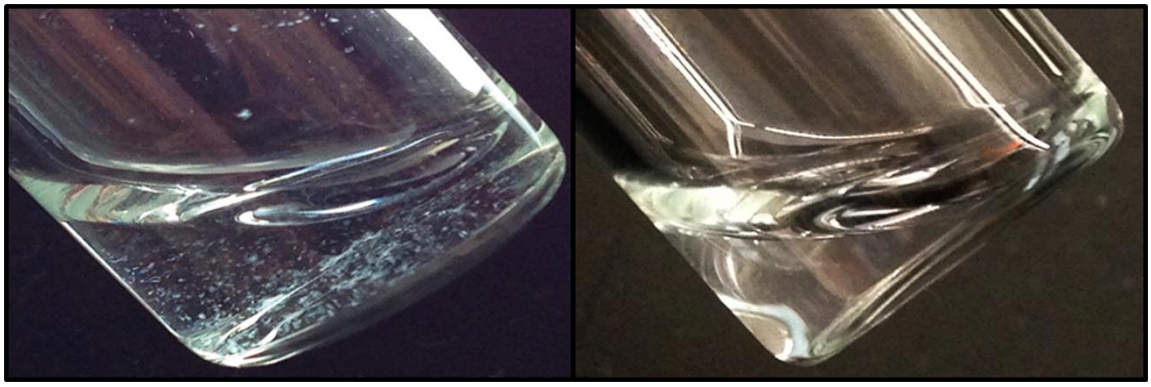

Figure 6. Aggregate formation ('white particulates') during native, unmodified ConA/PAH+ interaction (left) compared to PEGylated ConA/PAH+ interaction (right).

Glucose Response Study

PEGylated ConA was tested using a fluorescence anisotropy assay comprised of 200 nM APTS-MT (the competing ligand) and 1 μM PEGylated ConA to determine its effectiveness in tracking physiological glucose concentrations. Various concentrations of D-glucose (0 to ~800 mg/dL) were prepared in TRIS buffer and verified using an YSI

2300 Stat Plus biochemistry analyzer. A stock assay containing 2 μM mPEG-ConA and 400 nM APTS-MT was prepared in TRIS buffer. In a standard black 96-well microplate, 50 μL of the assay and 50 μL of the appropriate glucose concentrations were added to separate wells and mixed well. This created wells containing a final assay concentration of 200 nM APTS-MT and 1 μM PEGylated ConA with glucose concentrations ranging from 0 to ~400 mg/dL. Like before, the appropriate controls (TRIS buffer & 200 nM APTS-MT) were also added to separate micro-plate wells for baseline correction purposes. After time was given for the solutions to equilibrate (~10 min) at 22 ^{o}C, the steady-state anisotropy of each solution was measured with the TECAN Infinite F200 microplate reader.

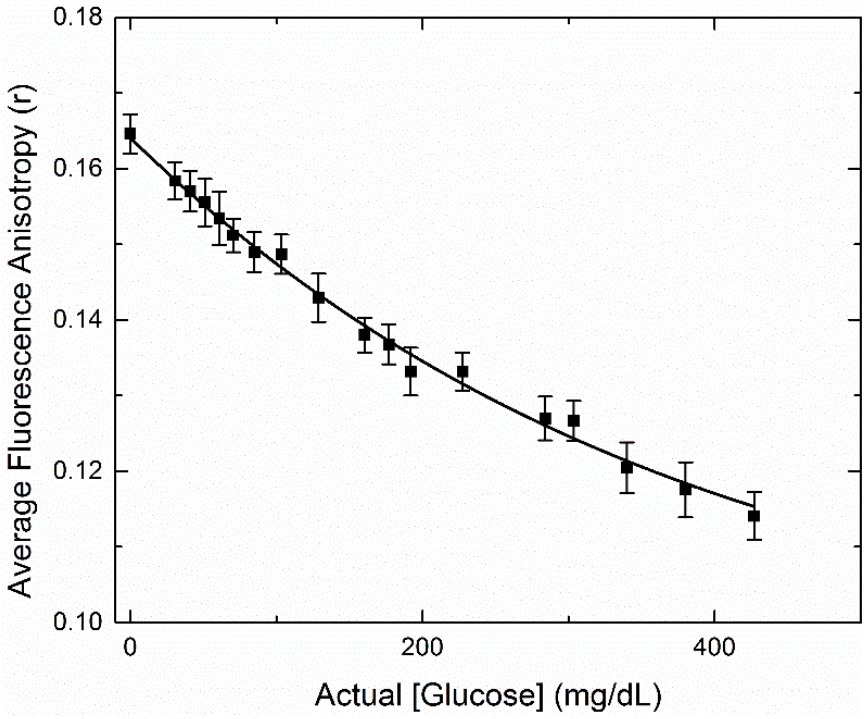

Figure 7. Glucose response of fluorescence anisotropy based assay using PEGylated ConA. The data was fitted to a standard competitive binding equation (solid line).

PEGylated ConA was expected to maintain its response to glucose because the binding of APTS-MT was not hindered by the presence of the PEG chains (Figure 4) and glucose (MW ~180 Da) is smaller than APTS-MT (MW ~1 kDa). To verify this, fluorescence anisotropy was used to track the behavior of an assay comprised of PEGylated ConA and APTS-MT in the presence of varying concentrations of glucose (Figure 7). This displays a characteristic competitive binding curve, where the anisotropy decreases in response to increasing glucose concentrations. This indicates that the PEGylation of ConA does not inhibit its ability to track physiological glucose concentrations in the competitive binding assay.

CHAPTER III

CHARACTERIZATION OF PEGYLATED CONA-MANNOTETRAOSE BASED ASSAY USING FRET AND COMPARISON OF EFFICIENY TO TRADITIONAL COMPETING LIGAND DEXTRAN*

Introduction

Herein, the PEGylated ConA and APTS-MT based assay is modified into a FRET based assay in order to develop a glucose sensing assay that can be implanted *in vivo*. The competing ligand, mannoteraose, is rationally-designed to present a single binding epitope (core trimannose) in close proximity to the signaling fluorophore, APTS. Using traditional, multivalent ligands for comparison (two different sized dextrans), we show that this new type of ligand improves the FRET efficiency upon binding to acceptor-labeled lectin. We then display that this enabling advantage improves the sensitivity of the assay to changes in physiological glucose concentrations (0 to 400 mg/dL) in comparison to the dextrans. Finally, we show that this new ConA-Mannotetraose based assay is thermally stable after incubation at body temperature (37 ^{o}C) for 30 days with a MARD of less than 10%.

FRET is a phenomenon where the energy of an excited fluorophore can non-radiatively transfer its energy to another fluorophore. With the properly chosen donor

* Part of this chapter is reprinted with permission from A.K. Locke, B. M. Cummins, and G. L. Coté. "High Affinity Mannotetraose as an Alternative to Dextran in ConA Based Fluorescent Affinity Glucose Assay Due to Improved FRET Efficiency," *ACS Sensors* **2016**, 1 (5), 584-590. Copyright 2016 American Chemical Society.

and acceptor fluorophores (overlapping emission/excitation spectra), the donor transfers its energy when the acceptor fluorophore is brought in close proximity (Equation 3). In this equation, E is the FRET efficiency, and R and Ro are the distance between the two fluorophores and the Forster radius, respectively.[66]

$$E = \frac{1}{1 + \left(\frac{R}{Ro}\right)^6}$$

Equation 4.

Labelling the competing ligand, mannotetraose, with the donor fluorophore (APTS) and the receptor, ConA with an acceptor fluorophore (TRITC), the assay is designed to induce FRET when complexes are formed. The equilibrium of these complexes shifts accordingly to changes in glucose concentration, and this shift can be tracked by measuring the ratio of the peak fluorescence intensities of the two fluorophores.

Determining the Binding Affinity of ConA Based Assay Using FRET

The binding affinity of the three different competing ligands to mPEG-TRITC-ConA was determined by tracking the fluorescence emission spectra during independent titration studies. First the competing ligands were synthesized as follows:

The synthesis of APTS-MT was performed using reductive amination and was previously discussed in detail.[28] Briefly, 13.5µL of 1 M APTS in acetic acid was added to ~1 mg of mannotetraose, allowing for the Schiff base intermediate to form between

the reducing terminus of mannotetraose and APTS. To stabilize this into a covalent bond, 13.5µL of 1 M sodium cyanoborohydride in tetrahydrofuran was added to the acetic acid mixture. This was well mixed and allowed to react at room temperature for 15 hr. The APTS-MT product was then purified via a HILIC column.

Two unique dextrans (MW: 70 kDa and 2 MDa) were labeled with APTS using the same reductive amination approach. Dex-2M allows for comparison with the proposed competing ligand due to similar binding affinities while Dex-70k is the most common competing ligand used in ConA based affinity assays. These fluorescent ligands (APTS-Dex-70k and APTS-Dex-2M) were synthesized using an APTS labeling kit from Prozyme®. Briefly, stock solutions of 50 mg/mL Dex-70k and 100 mg/mL Dex-2M were prepared in DI H_2O. Next, 10 µL and 20 µL of these solutions (Dex-70k and Dex-2M, respectively) were added to new centrifuge tubes. These solutions were centrifuged and then dried under a vacuum in a desiccator for 6 hours. Separately, the APTS reagent solution was then prepared by mixing the APTS solution (2.4 µL), APTS catalyst (6 µL) and reductant solution (2.4 µL) from the kit. Then, APTS reagent solution (4 µL) was added to each dried dextran samples and mixed well. These samples were sealed and placed in a water bath at 37 ^{o}C for 2 hours. After removing the solutions from the water bath, DI H_2O (500 µL) was added to each solution. The samples were then purified via 10 kDa centrifugal filters (Nanocep® from Pall) before passing through a GE Healthcare illustra MicroSpinTM G-25 column at ~3000 rpm for 2 minutes. An absorbance scan, from 240 nm to 600 nm, of the purified solution was taken via a Tecan® microplate reader to determine whether the sugar was conjugated to the dye.

The estimated number of dyes per dextran was calculated using the sulfuric acid based method designed by Albalasmeh *et al.* (Figure 8).[67]

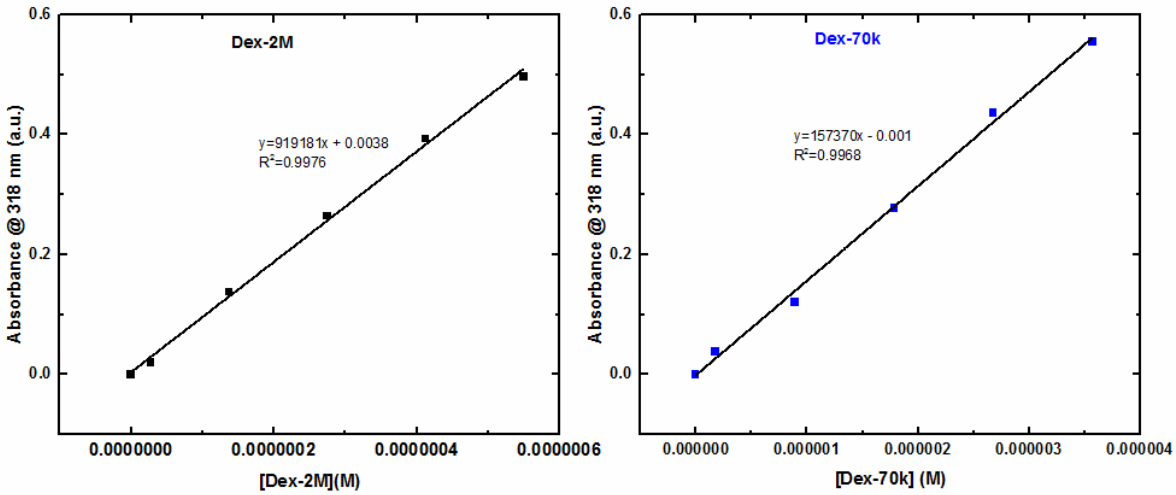

Figure 8. Calibration curve of the absorbance of (1) Dex-2M and (2) Dex-70k in the presence of sulfuric acid. The curves were used to estimate the concentration of each dextran after conjugation of APTS dye.

The synthesis of mPEG-TRITC-ConA has been previously described in detail. Briefly, 10 mg of TRITC-ConA was dissolved in ~1 mL sodium bicarbonate buffer. To occupy ConA's binding site, 2 mg of MaM was added to the protein solution. Next, ~25 mg of mPEG-NHS (5 kDa) was added to the solution for a molar concentration ratio of 16:1 mPEG to ConA. The solution was then continuously mixed for 6 hours. Afterwards, the solution was allowed to incubate for another 18 hours at room temperature without mixing. Dialysis against TRIS buffer removed MaM and unbound mPEG-NHS. The final concentration of mPEG-TRITC-ConA was determined by taking an absorbance scan from 240 nm to 640 nm using UV-Vis spectrometer.

Next, stock solutions of mPEG-TRITC-ConA (15.4 µM) and APTS-MT (10 µM) were first prepared separately in TRIS buffer. In a 1 cm path-length cuvette (C1), 1 mL of the assay (3 µM mPEG-TRITC-ConA and 200 nM APTS-MT) was prepared in TRIS buffer from the stock solutions. Fluorescence emission (475 nm to 650 nm) was measured with an ISS PC1 spectrofluorometer (λ_{ex} 450 nm). Subsequent emission scans were performed with the APTS-MT at the same concentration and decreased concentrations of mPEG-TRITC-ConA. Briefly, this was done by removing 500 µL of assay solution from C1 and adding 500 µL of 200 nM APTS-MT in TRIS buffer. This provided a new assay that comprised 200 nM APTS-MT and 1.5 µM mPEG-TRITC-ConA. The solution was mixed thoroughly and allowed to re-equilibrate before measuring the fluorescence spectra. This method was repeated to achieve final concentrations of mPEG-TRITC-ConA of: 750 nM, 375 nM, and 187.5 nM. Separate fluorescent scans of 1 mL APTS-MT (200 nM) and 1 mL mPEG-TRITC-ConA (3 µM) in TRIS buffer were taken under the same excitation conditions as the controls.

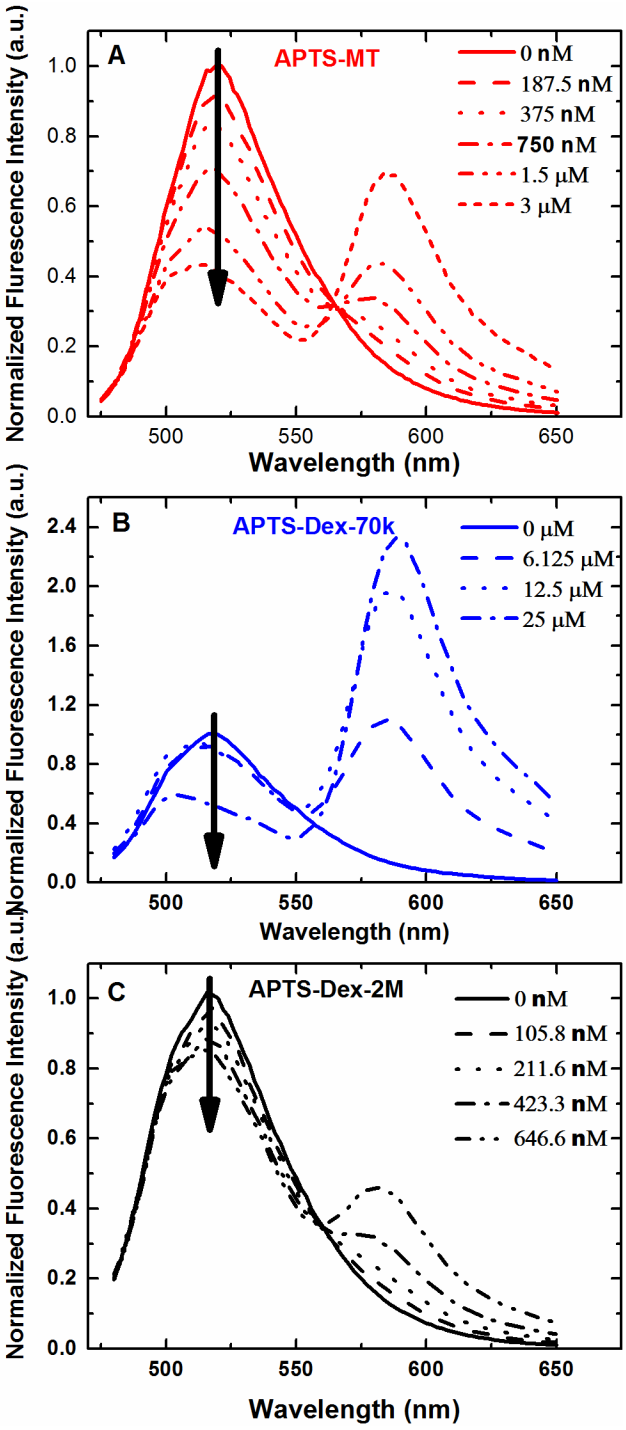

Figure 9. Titration curves comparing the change in fluorescence intensity of the different donor conjugated ligands: (A) APTS-MT, (B) APTS-Dex-70k and (C) APTS-Dex-2M; in response to in-creasing concentration of mPEG-TRITC-ConA (legend). All curves were normalized to the donor peak at 520 nm.

After all spectra were obtained from a given titration study (Figure 9), the fluorescence intensity at the peak emission for the donor fluorophore (i.e. APTS @ 520 nm) was plotted against mPEG-TRITC-ConA concentration. Each curve was then normalized to 1 at ConA=0 nM and fitted with Equation 4, giving the association constant to ConA ($K_a = 1/K_d$) for the given competing ligand (Figure 10). This fit also generated F∞, which is related to the efficiency of FRET transfer when the given competing ligand is bound to ConA.

$$F_{[ConA]} = \frac{1 - F_\infty}{1 + \frac{[ConA]}{K_d}} + F_\infty$$

Equation 5.

This method was repeated to determine the binding affinity of APTS-Dex-2M (52 nM) to mPEG-TRITC-ConA (0 to 850 µM). An attempt was made to perform this for APTS-Dex-70k however, the results were inconclusive. This is because it's affinity to ConA is too low to see an appreciable change in the donor fluorescence at these ConA concentrations.

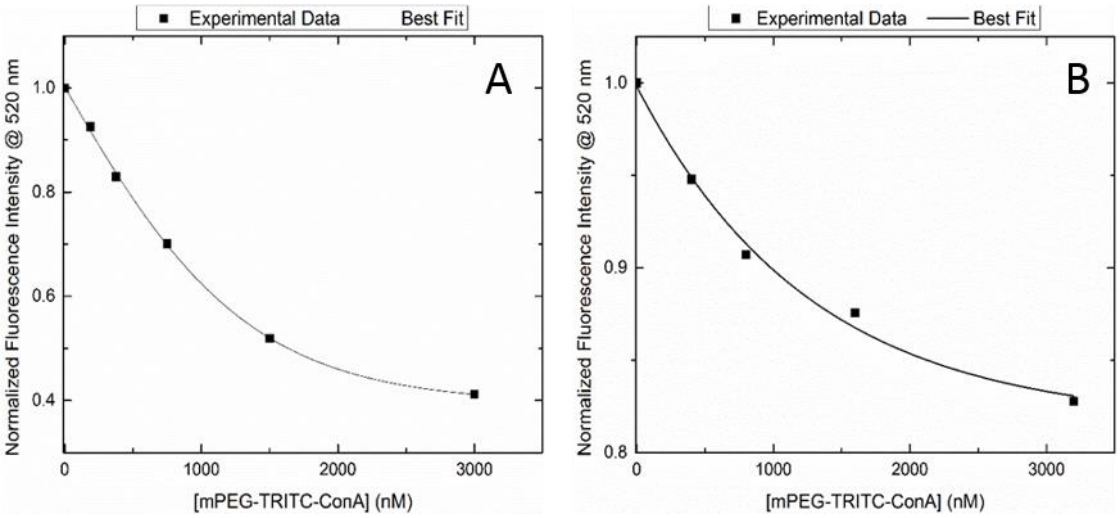

Figure 10. Normalized peak fluorescence intensity of APTS-MT fitted to a Boltzmann curve to determine the binding affinity of the FRET based assay containing (A) APTS-MT and (B) Dextran 2MDa as the competing ligand.

First, to ensure that the binding affinities were still comparable even after PEGylation, the titration curves generated previously were used to determine the K_a. The plot of the fluorescence intensity, at the donor peak, against increasing concentration of mPEG-TRITC-ConA was fitted with Equation 4 and the binding affinity was determined to be 3.2 x 10^6 M^{-1} and 2.61 x 10^6 M^{-1} for APTS-MT and APTS-Dex-2M, respectively. Benzeval reported a similar binding affinity of ~1.42 x 10^6 M^{-1} for Dex-2M binding to ConA and our previous fluorescence anisotropy work reported an affinity of approximately 5 x 10^6 M^{-1} for PEGlyated ConA-APTS-MT assay which validates our findings.[68] These K_a values are on the same order therefore we can assume that any difference in the fluorescence glucose response will be primarily due to the differences in the distance of the donor fluorophore (APTS) to the acceptor (TRITC) based on the structure and size of the competing ligands.

Comparing the FRET Efficiency of ConA Based Mannotetraose Assay Vs ConA Based Dextran Assay

The approximate FRET efficiencies for the different competing ligands when bound to ConA were calculated using the parameter from the previous fit (F_∞). Here, the value associated with the fluorescence of APTS-MT in the absence of ConA (100%) can be used as a control where there is no FRET transfer. The value associated with the fluorescence of APTS-MT in the presence of infinite ConA (F_∞) indicates the percentage of the original fluorescence from APTS-MT when all APTS-MT molecules in solution are bound to ConA. Therefore, using Equation 6 the average FRET Efficiency (E) when bound to ConA can be calculated for each competing ligand. The average distance (r) between the APTS and the TRITC when the competing ligand is bound to ConA can be approximated using Equation 7 and the calculated efficiencies and the approximate Forster Radius (R_0).[66]

$$E = 1 - F_\infty$$

Equation 6.

$$r = Ro\ \left(\frac{1}{E} - 1\right)^{\frac{1}{6}}$$

Equation 7.

The eventual performance of the competitive binding assay is dependent on the efficiency of FRET (E) when the donor-labeled competing ligand is bounded with the

acceptor-labeled ConA. This efficiency was evaluated for each APTS-labeled competing ligand using the parameters from the titration binding study.

APTS-MT is expected to have better FRET efficiency over the dextran based assays due to its size and the location of its single fluorophore on the competing ligand. The MW of mannotetraose is ~1 kDa compared to dextran (70 kDa and 2M Da). This much smaller size should ideally allow for its fluorophore to be brought closer in proximity to the fluorophores on ConA when bound compared to dextran.

The titration plots in Figure 9 show a greater change in fluorescence intensity for the APTS-MT based assay compared to the APTS-Dex-2M based assay; over slightly similar concentration range. After normalizing the fluorescence intensity at 520 nm and fitting it to equation 4, APTS-MT had a much higher FRET efficiency of ~89% compared to that of APTS-Dex-2M whose efficiency was determined to be ~25%. Furthermore, when compared to the traditional Dex-70k, APTS-MT also displayed improved efficiency. Moreover, due to its lower affinity, APT-Dex-70k required a much higher concentration range of the fluorescently labeled receptor required to obtain a very small and inconsistent FRET change making it difficult to determine its exact FRET efficiency.

The average distance between the two fluorophore in the absence of glucose was also calculated. FRET pair dyes APTS/TRITC have similar excitation and emission spectra to the commonly paired FITC/TRITC dyes. Therefore, their theoretical Forster Radius is expected to be similar and from the literature, FITC/TRITC is known to have an approximate Ro of 5 nm.[69] This Ro value and the FRET efficiency calculated

previously was used to calculate the estimated average distance between the bound and unbound APTS/TRITC based assay via Equation 6 and Equation 7; which was determined to be 3.5 nm and 6 nm, respectively for APTS-MT and APTS-Dex-2M.

Comparing the Glucose Response and Sensitivity of ConA Based Mannotetraose Assay Vs ConA Based Dextran Assay

The glucose responses of the different individual assays were measured by tracking the change in fluorescence intensity of donor and acceptor fluorophore. Using the binding affinities estimated above, the concentration of mPEG-TRITC-ConA was optimized using Equation 8 to allow for at least 50% of the assay to be in its bound state prior to the introduction of glucose.

$$\% B = \frac{[ConA]}{K_d + [ConA]}$$

Equation 8.

A stock glucose concentration of 39,500 mg/dL was prepared in TRIS buffer. In a cuvette, 1 mL of the assay solution (200 nM APTS-MT and 1 µM mPEG-TRITC-ConA) was prepared in TRIS buffer and mixed well. After giving sufficient time for the assay to reach equilibrium, the fluorescence emission was scanned (λ_{ex} 450 nm, λ_{ex}: 475-675 nm). Aliquots of the stock glucose were added to the assay to vary the glucose concentration across physiological concentrations. After each addition, the solution was mixed well and given sufficient time to equilibrate prior to scanning the fluorescence

emission in the same manner. Fluorescence scans were recorded for glucose concentrations that ranged from 0 mg/dL to 400 mg/dL. This was done in triplicate for the APTS-MT assay and repeated for assays based on the APTS-Dex-2M ligand (52 nM APTS-Dex-2M and 3 μM mPEG-TRITC-ConA) as well as assays based on the APTS-Dex-70k ligand (200 nM APTS-Dex-70k and 25 μM mPEG-TRITC-ConA) Higher concentrations of mPEG-TRITC-ConA were required in the APTS-Dex-70k assay because the affinity is lower for that competing ligand to bind to receptor. After the glucose-dependent fluorescence emission curves were obtained for each assay, the fluorescence intensity ratio (F_{520}/F_{600}) was calculated and plotted against the associated glucose concentration. The sensitivity of each assay was then calculated and compared. The data was then fitted to a Boltzmann curve to determine how well each assay can predict glucose concentration.

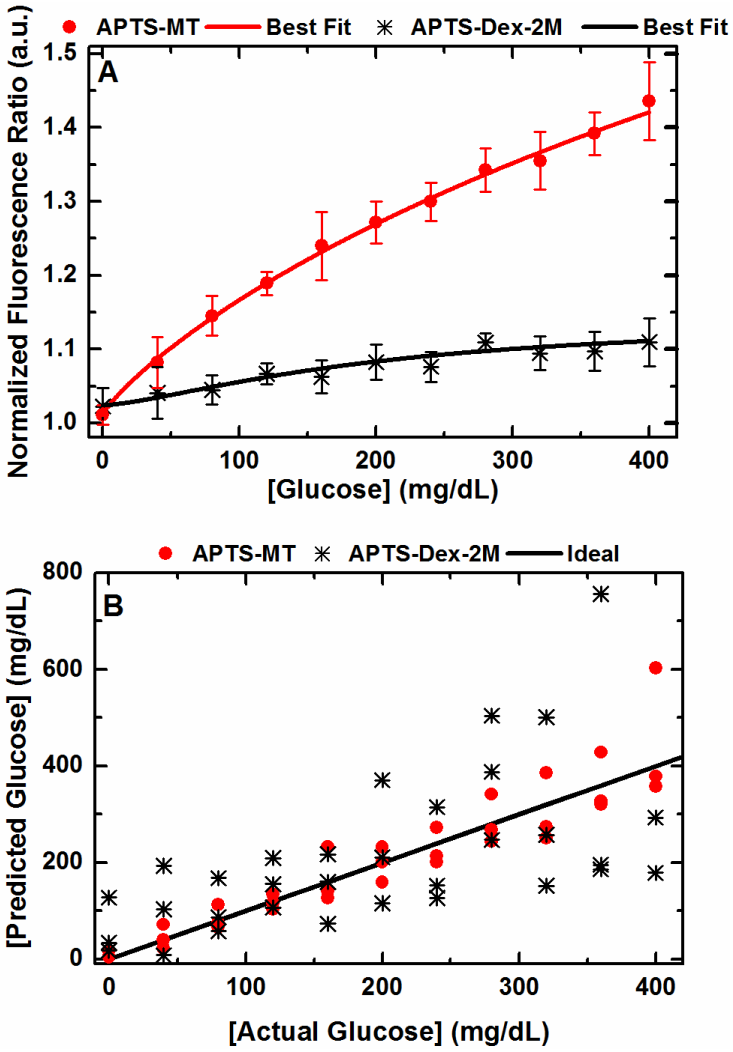

Figure 11. (A) The average glucose response of assays comprised 200 nM APTS-MT and 1 µM mPEG -TRITC-ConA showing improved FRET response and (B) predictability of glucose concentrations versus 52 nM APTS-Dex-2M and 1 µM mPEG-TRITC-ConA.

The performance of these two assays within the physiologically relevant glucose concentration range (0 to 400 mg/dL) was also evaluated in free solution at room temperature. (Figure 11). The results showed that the assay containing the fluorescently labeled monovalent ligand, APTS-MT, had a much greater FRET response to changes in

glucose concentrations. More importantly, APTS-MT was observed to be more accurate in predicting changes in glucose concentrations compared to APTS-Dex-2M. Furthermore, the average sensitivity of the assay to changes in glucose concentration was also calculated by determining the percent change in fluorescence ratio over the total glucose concentration range (%Δ F.ratio/mM). In free solution, the mannotetraose ($1.3 \pm 0.7\%$) based assay is approximately four times more sensitive to changes in physiologically relevant glucose concentrations than APTS-Dex-2M ($0.35 \pm 0.02\%$). Therefore, under the same conditions (i.e. same FRET pair fluorophores and temperature) the competing ligand mannotetraose appeared to have a better predictability and sensitivity to changes in glucose concentration than the dextran (2M). This may be due to the location of the fluorophore on these molecules. The size of mannotetraose allows the distance between its fluorophore and the fluorophore on the ConA to be in closer proximity than if the same fluorophore was on dextran; which contains multiple long branches terminated with the fluorophore. These multiple long branches therefore result in a less controlled placement of the fluorophore and in turn a less controlled distance between the donor and acceptor fluorophores compared to the mannotetraose based ligand. This in turn affects both the FRET efficiency and sensitivity of the assay resulting in the dextran based assay to be less efficient in predicting glucose concentrations.

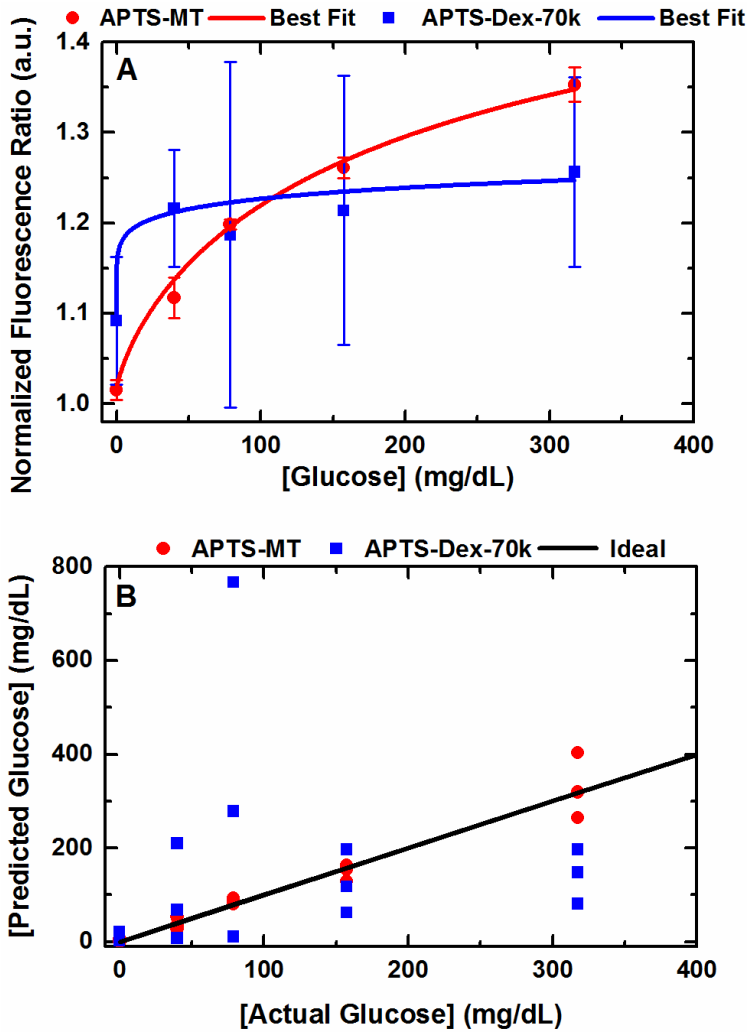

Figure 12. (A) The average glucose response of assays comprised 200 nM APTS-MT and 1 µM mPEG -TRITC-ConA showing improved FRET response and (B) predictability of glucose concentrations versus 52 nM APTS-Dex-70k and 25 µM mPEG-TRITC-ConA.

The glucose response of APTS-MT based assay was also compared to that of an assay comprised dextran with a MW of 70 kDa (Figure 12). This dextran is the most common dextran reported in literature for use in ConA based glucose sensing assays.[36] In literature, its binding affinity to ConA is reported to be ~15,000 M^{-1}.[18] Several research groups have shown this dextran to function within a ConA based glucose sensor

with good response to changes in physiological glucose concentrations, both *in vitro* and *in vivo*, when a substantial amount of ConA or dextran is used.[33] However, many have observed sensor failure over time with one possibility of the failure linked to aggregate formation between ConA and dextran. Therefore, previous work has shown that mannotetraose can act as a replacement for this competing ligand with improve functionality due to its non-aggregative behavior when interacting with ConA.[28]

It was observed that unlike APTS-Dex-2M the concentration of mPEG-TRITC-ConA had to be increase substantially in order to observe even the slightest change in FRET in response to glucose. This is due the Dex-70k's low K_a in a ConA based assay. For a dextran 70k based assay, for at least 50% of its molecules to be in the bound state, ~66 μM of ConA (note ConA solubility limit is 100 μM) is required compared to only 1 μM for a ConA-mannotetraose assay.

Herein, the mPEG-TRITC-ConA concentration which resulted in at least 25% of the molecules to initially be bound was used with hopes in minimizing aggregate formation between the two molecules which is also an issue with these ConA-Dextran based assays. It was observed that its change in fluorescence ratio is greater than dextran 2M with an approximate sensitivity of $0.7 \pm 0.1\%$ across the same physiological range. Chinnayelka *et al.* have also reported similar sensitivity of ~0.7% for a ConA-Dextran 70k based FRET assay in free solution.[70] However, when compared to APTS-MT, the mannotetraose based assay still had improved sensitivity and reproducibility (note the large error bars for APTS-Dex-70k assay) in response to changes in glucose concentration overall. The concentration of the competing ligand could have also been

increased in these experiments. However, the ideal sensor should be sensitive to lower glucose concentrations, which requires very low concentration of the competing ligand.

Glucose Response under Thermal Conditions

The glucose response of an assay containing mannotetraose at 37 ^{o}C was evaluated after 30 days to determine the assay's stability and activity under physiologic thermal conditions (Figure 13). Results show that the MARD% over the hypoglycemic range (< 70 mg/dL) was ~9%, the euglycemic range (i.e. between 70 and 180 mg/dL) was 2% and the hyperglycemic range (<180 mg/dL) was ~4%. The overall MARD between 0 and 400 mg/dL was ~5%.

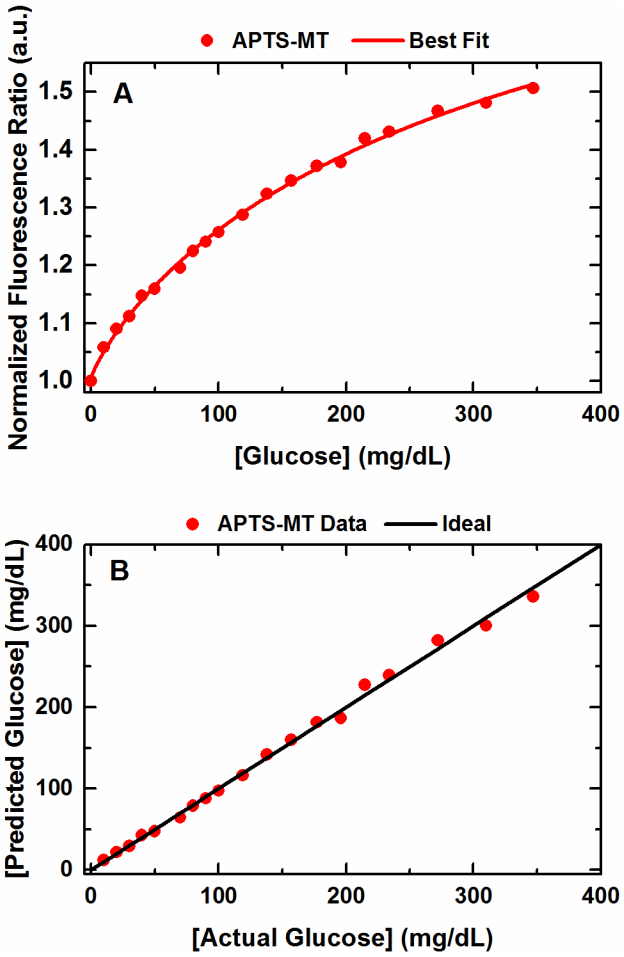

Figure 13. (A) Normalized fluorescence ratio of assay composed of ConA-MT and (B) predicted versus actual glucose response of same assay indicating the assay's ability to predict changes in glucose concentrations with a MARD of less than 10% after 30 days incubation at 37 ºC.

CHAPTER IV

ENCAPSULATION OF ASSAY WITHIN BIOCOMPATIBLE AMPS PNIPAAM HYDROGEL

Introduction

Previous chapters introduced a thermally stable, non-aggregative glucose sensing assay comprised mPEG-TRITC-ConA and APTS-MT. Thus far, this assay has only been evaluated in free solution. Therefore, within this chapter this assay is encapsulated within the biocompatible membrane AMPS-PNIPAAm, developed at Texas A&M University by Dr. Melissa Grunlan's research group, and evaluated for its functionality as a glucose biosensor.

PNIPAAm is a hydrogel that is synthesized via copolymerization of *N*-isopropylacrylamide and a crosslinker *N, N'*-methylenebisacrylamide (BIS). In its traditional form, as a single network (SN) hydrogel, PNIPAAm is able to slowly switch between a swollen (hydrophilic) and deswollen (hydrophobic) state in response to a thermal stimulus around its volume phase transition temperature (VPTT) of ~33-35 ^{o}C.[71] This mechanical change due to the thermal stimuli has made these hydrogels useful for biological applications such as protein and cells detachment for tissue engineering, anti-fouling coatings and self-cleaning membranes. To improve on its mechanical strength and rate at which the membrane swells and deswells, various modification of the fabrication method have been employed such as the addition of nanocomposites, the synthesis of double network hydrogels and the addition of comonomers.

Double network (DN) PNIPAAm hydrogels are known to be more mechanically robust. These hydrogels consist of interpenetrating polymer networks of two different degrees of cross-linked network. The enhanced mechanically properties that these gels provide can allow these hydrogels to be used as biocompatible, "self-cleaning", implantable membranes that would stimulate little to no fibrous encapsulation by the immune response. Fei *et al.* introduced DN PNIPAAm hydrogels containing polysiloxane particles used to enhance the hydrogel's thermosensitivity without altering its VPTT.[72] Also, to shift the VPTT to ~38 ^{o}C which would allow for the membrane to be in the swollen hydrophilic state when implanted in the body, *N*-vinylpyrrolidone (NVP) comonomer was introduced into the fabrication of these DN hydrogels.[73, 74] Cell release studies have shown the detachment of cells of the surface of these modified DN hydrogels when the membrane is thermally cycled around body temperature.[73] Furthermore, the glucose diffusion coefficient at body temperature (35 ^{o}C) through these membranes are ~ 1.88 $\pm$ 0.01 x 10^{-6} cm^2/s which is comparable to the diffusion coefficient of glucose diffusion through the dermis and slightly faster than the diffusion through the epidermis.[73, 75]

Recently, the DN PNIPAAm hydrogels were redesigned to replace the polysiloxane particles with AMPS because the particles only improved the thermosensitivity but not the hydrogel's mechanical properties, with AMPS. Fei *et al.* showed that the inclusion of AMPS demonstrated improved both the thermosensitivity as well as the mechanical properties.[76] Furthermore, the addition of the AMPS comonomer provided an overall negative charge of the membrane.[76] This modified

hydrogel was evaluated *in vitro* and the incorporation of 25% AMPS and 75% AMPS were shown to be more favorable in disallowing cells to attached to its surface.[77] Moreover, the glucose diffusion through these hydrogels at body temperature remained relatively unaffected at $1.99 \pm 0.01 \times 10^{-6}$ cm^2/s for 25% AMPS hydrogels and slightly faster for 75% AMPS which exhibited a glucose diffusion coefficient of $2.21 \pm 0.02 \times 10^{-6}$.[77]

Herein, 25% AMPS-PNIPAAm hydrogel was chosen for the use as the biocompatible housing chamber for the glucose sensing assay because of easy fabrication into a rod shape and concerns the biocompatibility of highly electrostatic charged materials in the body. However, in terms of encapsulation of nanoscale particles such as the glucose sensing assay, the large pores of hydrogels (60-200 μm) are problematic. This chapter aimed to show that directly injecting the assay into the AMPS-PNIPAAm hydrogel rods would result in a decrease in FRET signal, in response to glucose, due to leaching of the assay from the hydrogel and thus resulting in the failure of sensor to sense glucose. Therefore, in order for AMPS-PNIPAAm to be used as a housing chamber for the glucose sensing assay various encapsulation techniques such as Layer by Layer, microspheres encapsulation or membrane immobilization needed to be employed in order to minimize leaching of the assay from the PNIPAAm membranes without greatly impacting glucose diffusion into the assay's surroundings.

Synthesis of AMPS PNIPAAm Hydrogel Rods for Encapsulation

The hydrogel rods were formed through a two-step, in situ photo-cure process. The single network (SN) copolymer precursor solution was synthesized with NIPAAm monomer, AMPS monomer (75:25 wt% NIPAAm:AMPS), BIS crosslinker, Irgacure-2959 photoinitiator and DI H_2O. In a 50 mL round bottom (RB) flask equipped with a teflon-covered stir bar, NIPAAm & AMPS (total weight of 1.0 g), BIS (0.04 g), and Irgacure 2959 (0.08 g) were dissolved in DI H_2O (7.0 mL). The double network (DN) precursor solution was formed by combining NIPAAm (6.0 g), NVP (0.96 g), BIS (0.012 g), Irgacure 2959 (0.24 g), and DI H_2O (21.0 mL). SN cylindrical hydrogels with a hollow center (outer diameter = 1 mm, inner diameter = 0.3 mm, length = 10 mm) were prepared by pipetting the SN precursor solution into a cylindrical glass mold (outer diameter = 1 mm, length = 10 mm) fitted with Teflon end caps and steel wire (diameter = 300 µm, inserted through the center of the caps) to create a centered hollow inner cavity. The mold was immersed in an ice water bath and exposed for 30 min to longwave UV light (UV-transilluminator, 6 mW cm^{-2}, 365 nm). To remove hydrogels, Teflon caps were detached and molds were heated in the oven for ~20 min at 120 °C to dehydrate gels enough in order for them to slide out of the molds without fracture. The SN hydrogels were soaked in DI H_2O for 2 days at RT and then transferred into the DN precursor solution to soak for 2 days at 2 °C. Next, a steel wire (diameter = 500 µm) was inserted into the hollow cavity of each cylindrical hydrogel (diameter larger due to swelling). The hydrogels were individually wrapped in transparent plastic wrap (Saran™) then submerged in an ice water bath, exposed for 10 min to longwave UV

light, and soaked in DI H_2O as above. A clean razor blade was used to trim ends to achieve a final geometry of 5 mm x 2.5 mm x 600 μm (length x outer diameter x inner diameter).

Synthesis of AMPS PNIPAAm Hydrogel Membrane for Glucose Diffusion Studies

The cylindrical membranes were formed through a two-step, in situ photo-cure process. The SN copolymer precursor solution was formed with NIPAAm monomer, AMPS monomer (75:25 wt% NIPAAm:AMPS), BIS crosslinker, Irgacure-2959 photoinitiator and DI H_2O. In a 50 mL RB flask equipped with a teflon-covered stir bar, NIPAAm & AMPS (total weight of 1.0 g), BIS (0.04 g), and Irgacure 2959 (0.08 g) were dissolved in DI H_2O (7.0 mL). The DN precursor solution was formed by combining NIPAAm (6.0 g), NVP (0.96 g), BIS (0.012 g), Irgacure 2959 (0.24 g), and DI H_2O (21.0 mL). SN rectangular sheet hydrogels were prepared similarly by pipetting the SN precursor solution into a rectangular mold consisting of 2 glass slides separated by 1 mm thick Teflon spacers. The mold was immersed in an ice water bath and exposed for 30 min to UV light. The SN hydrogel was removed from the mold, soaked in DI H_2O for 2 days, and then transferred into the DN precursor to soak for 2 days at 2 °C. The gels were then sandwiched between 2 glass slides with 1 mm thick Teflon spacers enclosing the edges for support. The molds were immersed in an ice water bath and exposed for 30 min to UV light. The DN hydrogels were removed from the mold and soaked in DI H_2O as before. Final dimensions for the glucose study is 1 cm x 1 cm x 1 mm (length x width x thickness).

Encapsulation of Assay

Different encapsulation techniques such as calcium carbonate, alginate microspheres and direct embedding via LbL were investigated to determine the encapsulation strategy that resulted in high loading efficiency, glucose diffusion/response and assay retention. Increasing the size of the competing ligand via PEGylation was also investigated to try and retain the assay components within the hydrogel rods.

Direct Encapsulation

The assay (10 µM mPEG-TRITC-ConA and 2 µM APTS-MT) was directly encapsulated into the AMPS-PNIPAAm hydrogel rods (~ 5mm in length) by pipetting 1 µL of the assay into the hollow cavity and the ends were sealed with glass bead (710-850 microns; Cospheric LLC) coated with ~98 wt% PEG (MW 575). The assay containing rods were then placed in wells of a 96 well-plate (Grenier, flat transparent) and a Tecan® Microplate reader was used to measure the FRET response in the presence of high concentration glucose (~1000 mg/dL).

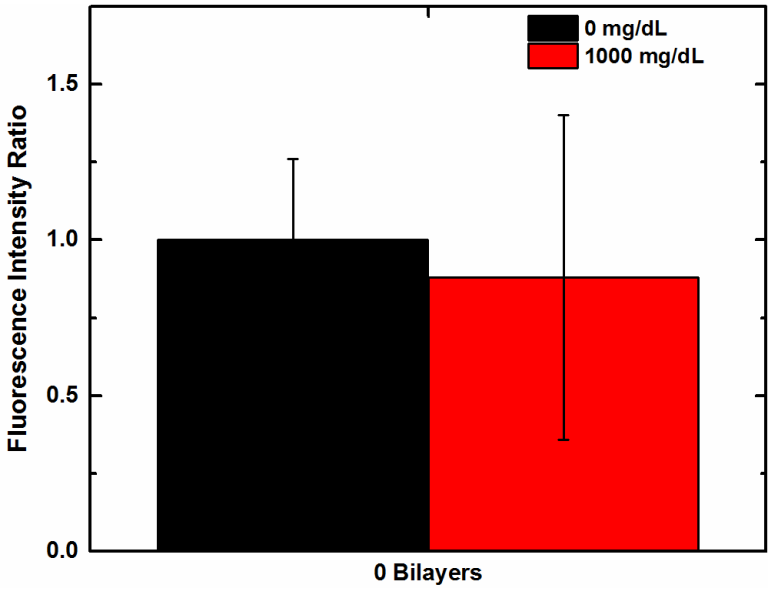

Figure 14. The average glucose response of three FRET based biosensors after direct encapsulation of the assay (comprised 2 µM APTS-MT and 10 µM mPEG -TRITC-ConA) in the AMPS-PNIPAAm rods indicating failure and inconsistency of the sensor to respond to high concentration of glucose due to leaching of assay components.

Results showed that direct encapsulation of the assay resulted in a decrease in the FRET signal when glucose was introduced (Figure 14). This indicated failure of the sensor and it is due to the leaching of the assay components from the hydrogel membrane when glucose is introduced. The introduction of glucose replaced

APTS-MT at ConA's binding site allowing the small molecules to be in its free state and due to size (~1 kDa; < 1nm) can then easily diffuse out of the membrane.

Therefore there is a need to either increase the size of the assay or design a technique to indirectly encapsulate the glucose sensing assay either via the use of microspheres or modification to the AMPS-PNIPAAm membrane via LbL.

Calcium Carbonate Microspheres

Layer by Layer deposition on calcium carbonate microsphere is one of the most commonly used method for various applications such as assay encapsulation for the design of nano/microsensors and drug delivery.[78] This technique is desirable due to the easy fabrication method, high surface area, and easy dissolution of template under mild conditions and neutral pH; which would cause little to no harm to encapsulated materials such as proteins.[79] Typically, calcium carbonate spheres self-assembles via co-precipitation during the reaction of calcium chloride and sodium carbonate. Polyelectrolyte layers of alternating opposite charge can then be deposited on the surface of these spheres; which can function as both a housing chamber for the content being trapped and as a semi-permeable membrane for the diffusion of desired analytes into the spheres.[80] After the deposition of the desired amount of layers, the core can then be removed by either ethylenediaminetetraacetic acid (EDTA), 2-ethanesulfonic acid (MES) or hydrochloric acid (HCl) which dissolves calcium carbonate into calcium ion and carbonate by-products.

Therefore, because of the simplicity of the fabrication method and the advantage of utilizing the layers as a diffusion membrane for glucose, this technique was investigated for the encapsulation of the glucose sensing assay.

The LbL calcium carbonate microspheres where fabricated based on previous work published by Dr. Michael McShane's lab at Texas A&M University, where MES buffer was shown to be more effective in chelating the calcium core due to its low pH.[81] Furthermore the (PVSA) poly (vinyl sulfonic acid) was used in the fabrication method to

produce stable vaterite polymorph calcium carbonate spheres; which are said to be more water soluble and easier to dissolve.[81] However, because ConA is a protein, this MES buffer may have an effect on denaturing the protein or deactivating its binding site. Therefore, the activity of mPEG-ConA was first investigated to ensure that the MES buffer would fully dissolve the core without affecting the binding functionality of the protein.

Briefly, mPEG-ConA in 0.2 M Na_2CO_3 buffer (1 mL) was added to a beaker and stirred at 800 RPM for 1 min. Next, 1 mL of 0.2M $CaCl_2$ was quickly added to the solution and after 1 min the speed was reduced to 600 RPM. After 10 min, 50 µL of poly (vinyl sulfonic acid) PVSA was added and stirred for another 5 min. The particles were then spun down at 1000g for 2 min and the supernatant was removed. To determine the activity of the encapsulated mPEG-ConA, the $CaCO_3$ was dissolved by washing the microspheres two times in a 3K Microsep with 0.25 M MES buffer (pH 6.1). Three more washes were then performed with TRIS buffer. The concentration of mPEG-ConA was determine via absorbance at 280 nm measured on UV-VIS spectrometer. Fluorescence anisotropy, conducted similar to before, was then used to determine the binding affinity of the mPEG-ConA to APTS-MT (Equation 3).

Results showed that the binding affinity of the encapsulated mPEG-ConA was 7.41×10^6 M which is similar and on the same order to the binding affinity reported in previous work.[82] Therefore, the affinity was not significantly affected when MES buffer was used to chelate the calcium core. This was further verified via scanning electron microscopy/energy dispersive X-ray spectroscopy (SEM/EDX) image in Figure 16

which showed no presence of calcium residues after the dissolution of the calcium carbonate core (Figure 16).

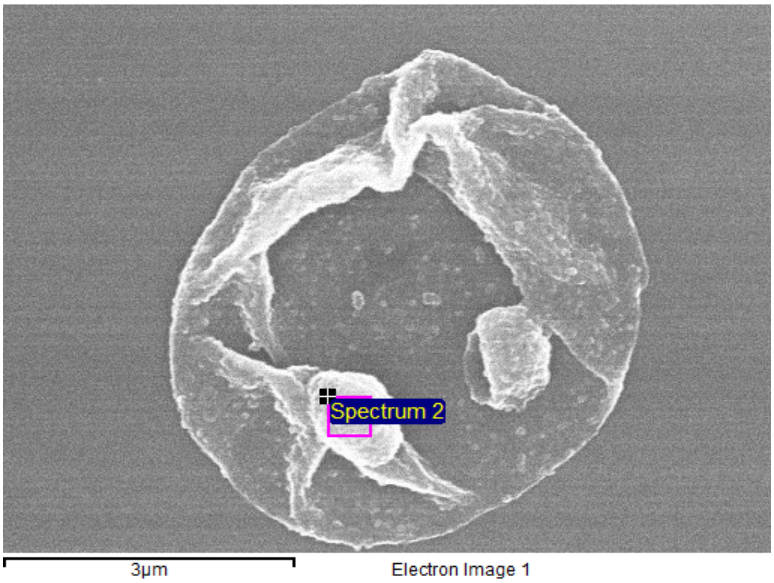

Figure 15. Scanning electron microscopy image of LbL calcium carbonate microspheres after treatment with MES buffer to remove calcium carbonate core. The collapsed walls indicate the absence of the core.

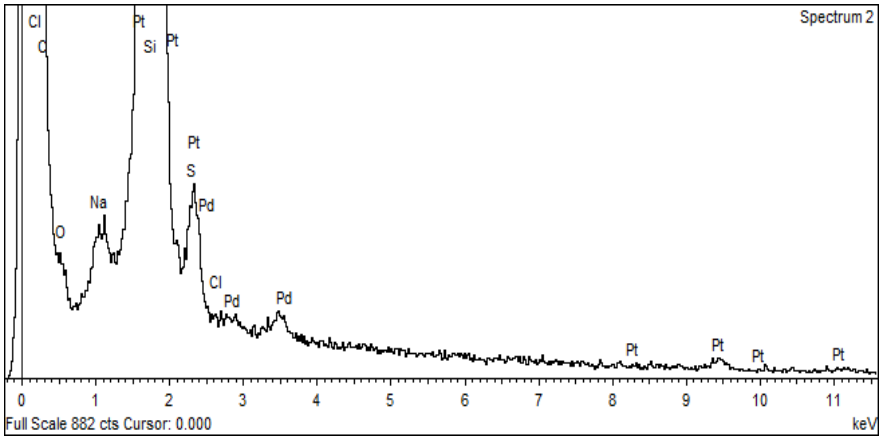

Figure 16. Energy dispersive X-ray spectrum indicating the absence of calcium ions confirming the removal of the calcium carbonate core after treatment with MES buffer.

Next, the complete FRET based glucose sensing assay was encapsulated within LbL $CaCO_3$ microspheres. The $CaCO_3$ microspheres were prepared similar to above with the 1 mL of the assay (23 µM mPEG-TRITC-ConA and 400 nM APTS-MT) dissolved in Na_2CO_3 buffer. Before the core was dissolved with MES buffer, eight bilayers of $PDADMAC^+/PSS^-$ were deposited on the surface of the microspheres in order to create a semi-permeable membrane that would retain the assay but allow glucose to diffuse into the core. Then similar to before, the $CaCO_3$ microspheres core was dissolved by washing the microspheres three times in a 3K Microsep with 0.25 M MES buffer (pH 6.1). The spheres were re-suspended in TBS buffer. Fluorescence microscopy images (Figure 17) confirmed that both assay components were distributed throughout the LbL calcium carbonate templated microspheres (~ 3µm).

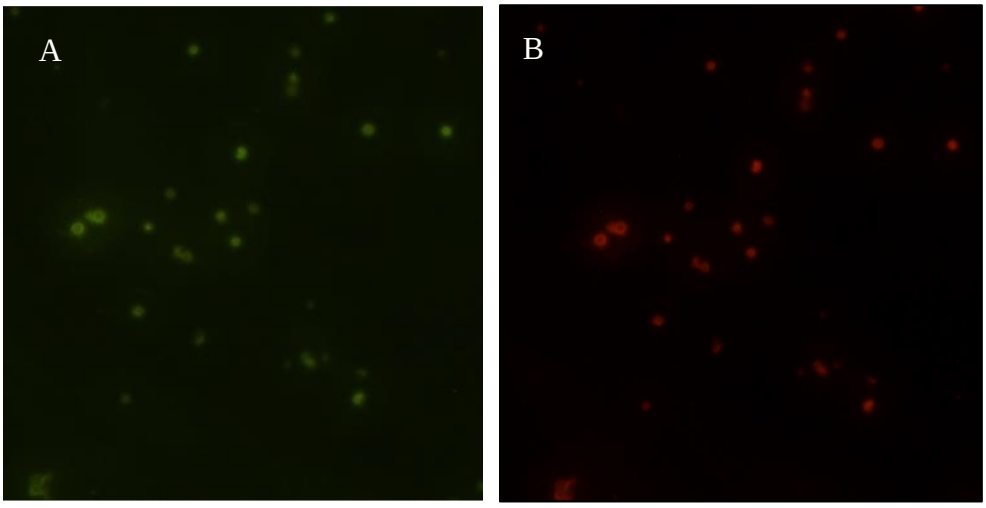

Figure 17. Fluorescence images of the assay (A) APTS-MT and (B) mPEG-TRITC-ConA after encapsulation in ~ 3 µm LbL calcium carbonate templated microspheres.

To test the performance of the microspheres within the AMPS-PNIPAAm hydrogel rods, the microspheres were pipetted into the hollow AMPS-PNIPAAm rods (~ 5 mm in length) and packed to capacity (~1 µL volume of spheres). The rods were then capped with glass beads coated in ~98 wt% PEG (MW 575). The glucose response data showed a change in FRET signal of ~16% with increasing glucose concentration from 0 mg/dL to 400 mg/dL.

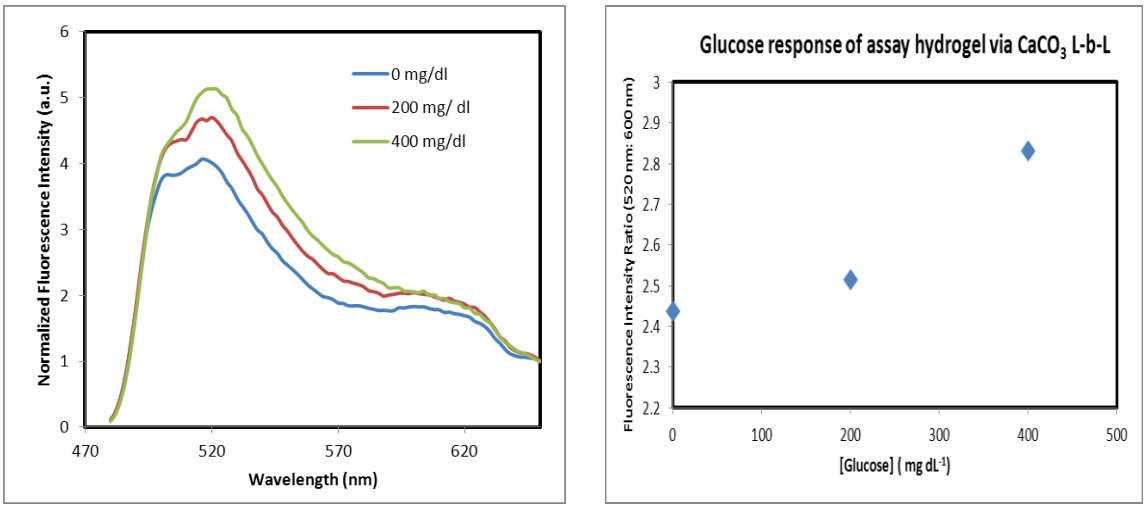

Figure 18. FRET response of the assay encapsulated within LbL calcium carbonate templated microspheres indicating a change in FRET signal in the prescence of varying concentration of glucose within the physiological relevant range.

Although promising, these results were not repeatable (Figure 19) within the same batch of microspheres. This may be due to inhomogeneity issues. Also another limitation is the high initial concentration of assay required and an estimated low loading efficiency (less than 15%).

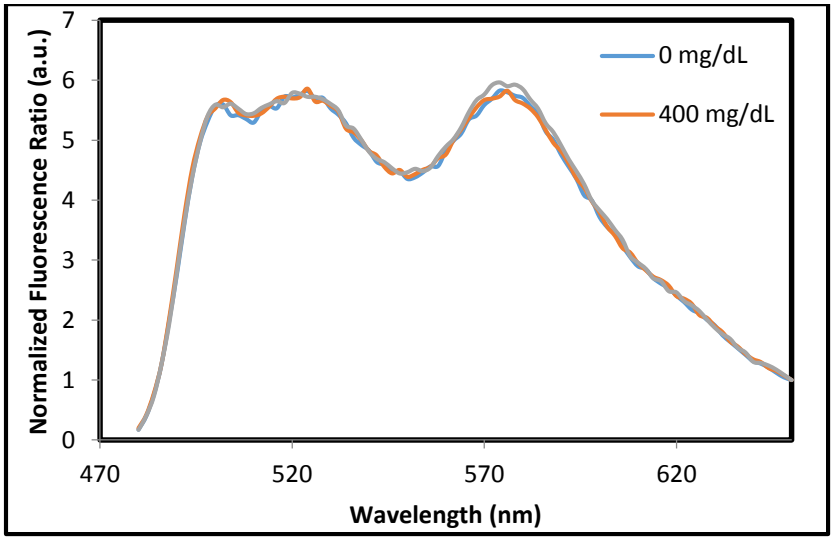

Figure 19. Repeated FRET response from the same batch of the assay encapsulated within LbL calcium carbonate templated microspheres indicating no change in FRET signal in the prescence of varying concentration of glucose within the physiological relevant range.

Alginate Microspheres

Another commonly used encapsulation method for the design of biosensors is alginate LbL microspheres. Different research groups have utilized this method for the encapsulation of fluorescence based sensing assays due to its easy and mild fabrication method which would result in little to no harm to sensitive molecules such as proteins.[83, 84] Therefore this technique was investigated next as a potential indirect microencapsulation of the glucose sensing assay. The assay containing microspheres were fabricated by Dr. Michael McShane's research group at Texas A&M University.

Briefly, 500 µL of the glucose sensing assay (10 µM mPEG-TRITC-ConA and 2 µM APTS-MT) in TBS was mixed with 3.8 mL alginate solution (3%). This solution was then added to 7.5 mL of Span-85/iso-octane solution and allowed to mix via a

homogenizer at 8,000 RMP for two minutes. Next, 1 mL of TWEEN-85 solution was added to the emulsion and allowed to continue mixing for another minute. Calcium chloride solution (10% w/v) was then pipetted into the emulsion and the homogenizer was turned off. The emulsion was then transferred to an RB flask and allowed to mix on a magnetic stir plate for 20 minutes. The particles were then spun down at 2000g to form a pellet. The supernatant was then removed and the particles were washed three times with DI H_2O. Immediately following synthesis, 10 bilayers of PAH^+/PSS^- was deposited on the microspheres surface using standard LbL technique. The assay containing alginate calcium LbL microspheres were then re-suspended in TBS.

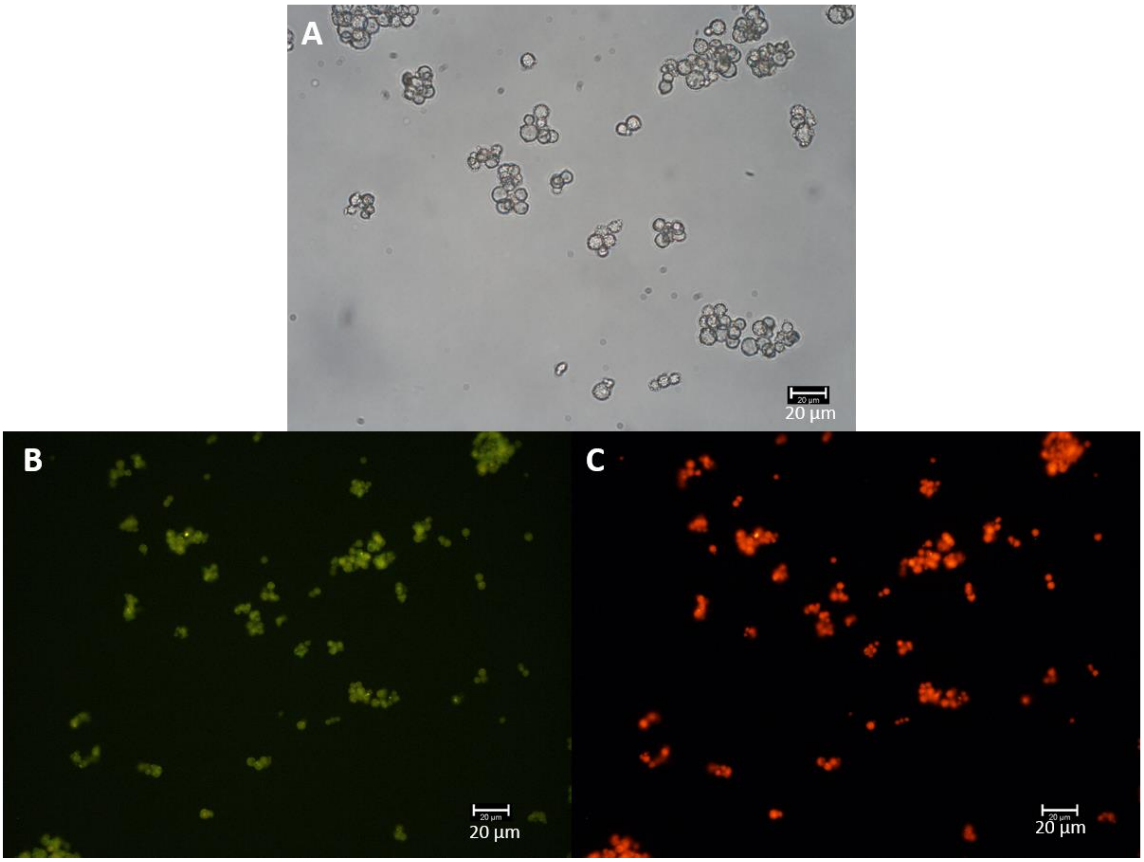

Figure 20. (A) Bright-field and Fluorescence images of the assay (B) 2 µM APTS-MT and (C) 10 µM mPEG-TRITC-ConA after encapsulation in LbL alginate-calcium microspheres.

The fluorescence images showed that assay contained within the microspheres which had an average diameter of 5 to 10 µm (Figure 20). To test the glucose response, different volumes of spheres (10 µL, 20 µL, 50 µL and 100 µL) in TBS were pipetted into a 96 well-plate (Corning) and fluorescence emission measurements were taken from 480 nm to 680 nm with an excitation of 450 nm. Next, glucose was added to each well for a final concentration of 600 mg/dL and fluorescence measurements were taken after 30 minutes of incubation.

Once again the glucose response data showed little to no change in FRET signal; less than 3% across physiological relevant glucose range (Figure 21). Furthermore, the high concentration of assay required and unknown loading efficiency due to high dilution factor made it difficult to optimize the fabrication method to try and improve the FRET efficiency.

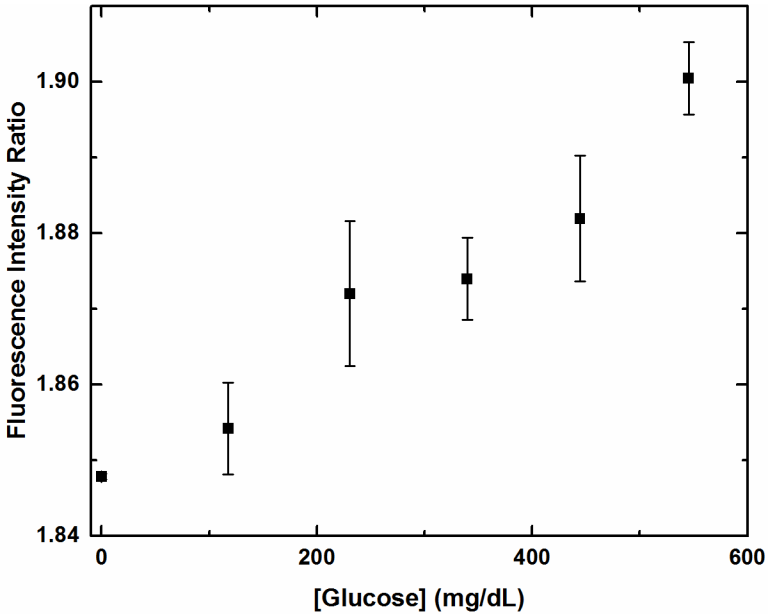

Figure 21. The average FRET response of the assay encapsulated within LbL alginate-calcium microspheres indicating little to no change in FRET signal in the prescence of varying concentration of glucose within the physiological relevant range.

Increasing APTS-MT Size via PEGylation

The size of APTS-MT is ~1 kDa (< 1 nm), therefore to increase its size and the potential for it to be retained within the biocompatible membrane the technique of PEGylation was explored. The fluorophore APTS has three potential functional groups

(3x sulfonyl chloride) that can be utilized for the conjugation of short PEG chains (Figure 22).

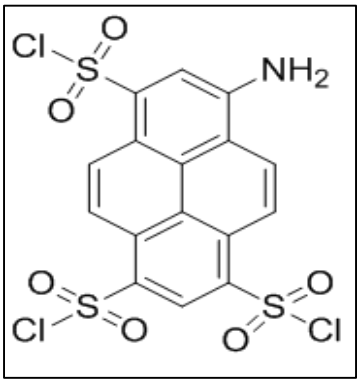

Figure 22. Schematic of the native structure of the donor fluorophore, 8-aminopyrene-1, 3, 6-trisulfonyl chloride.

The synthesis of this bulked up APTS-MT was conducted by Dr. Gabbai's research group at Texas A&M University. Briefly, PEG chains (MW 2 kDa) were attached to the fluorophore based on the following reaction where 0.015 mmol of the dye (compound 1) was dissolved in CH_3CN (0.50 mL) followed by the addition of a 0.046 mmol PEG-amine (H_2N-PEG) and 0.057 mmol disopropylethylamine (DIEA) (Figure 23). The solvent was then removed under reduced pressure and the residue was redissolved in DI H_2O (1.00 mL).

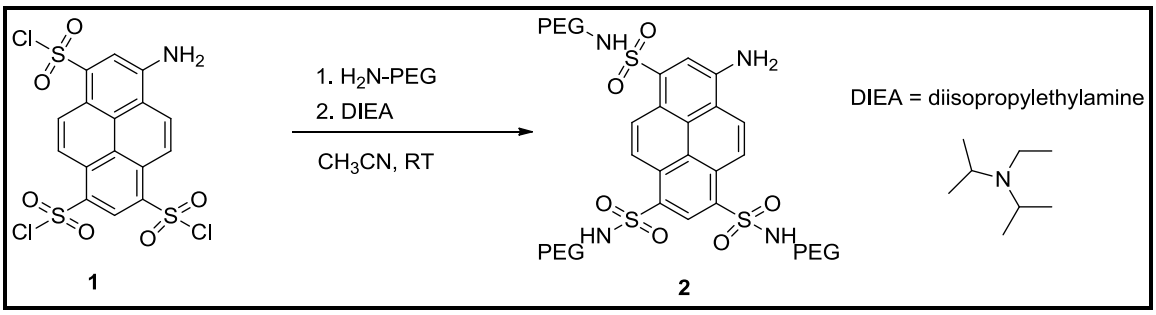

Figure 23. Synthesis of PEGylated APTS to increase the size of the competing ligand by increasing the apparent size of the donor fluorophore via the addition of three PEG chains (MW 2 kDa).

The excess PEG-amine was removed via dialysis and absorbance was used to confirm the presence of the PEG chains (Figure 24). It is expected that the addition of each PEG chain would result in ~7 to 10 nm wavelength redshift. A 50 nm wavelength shift was observed after the addition of the PEG chains to the dye (Figure 24). This confirmed the presence of the PEG chains.

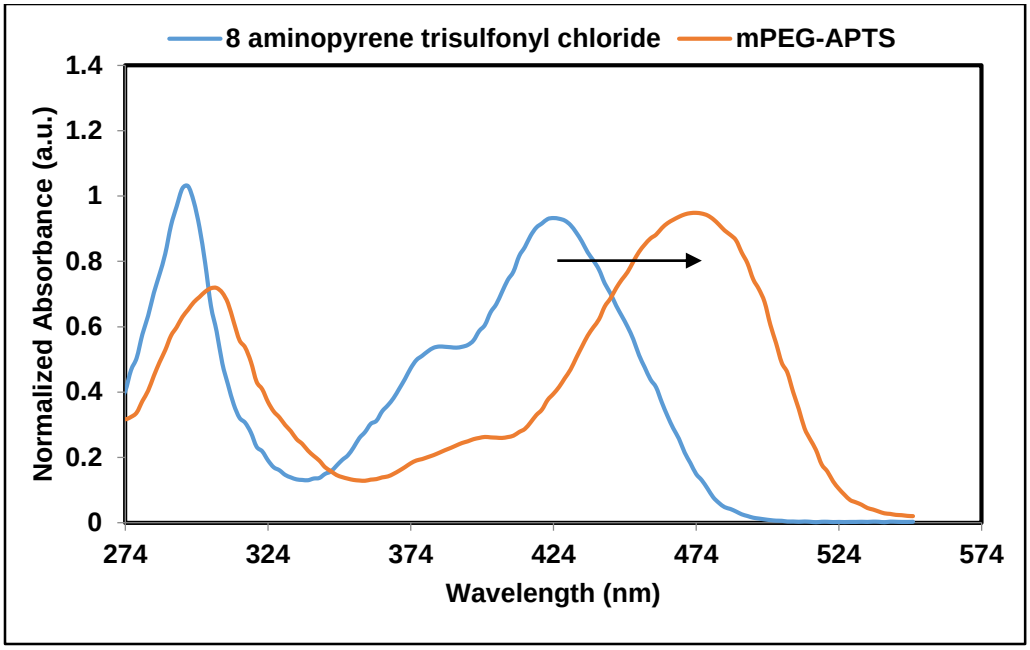

Figure 24. Absorbance spectroscopy scan indicating an approximate 50 nm wavelength shift after the addition of the PEG chains.

Following the conjugation of the dye, mannotetraose was conjugated to the free aromatic amine group on the newly PEGylated dye (Figure 25). Briefly, 0.0010 mmol of the PEGylated dye was dissolved in 15% acetic acid (AcOH) aqueous solution (0.20 mL). Next, 0.0015 mmol of mannotetraose was added to the solution and 0.50 mL of 15% AcOH aqueous solution was added to the mixture. The solution was then stirred at room temperature for 10 min and then 0.0160 mmol sodium cyanoborohydride ($NaBH_3CN$) dissolved in 0.30 mL tetrahydrofuran (THF) was added to the mixture. The reaction mixture was then stirred at room temperature for 15 h.

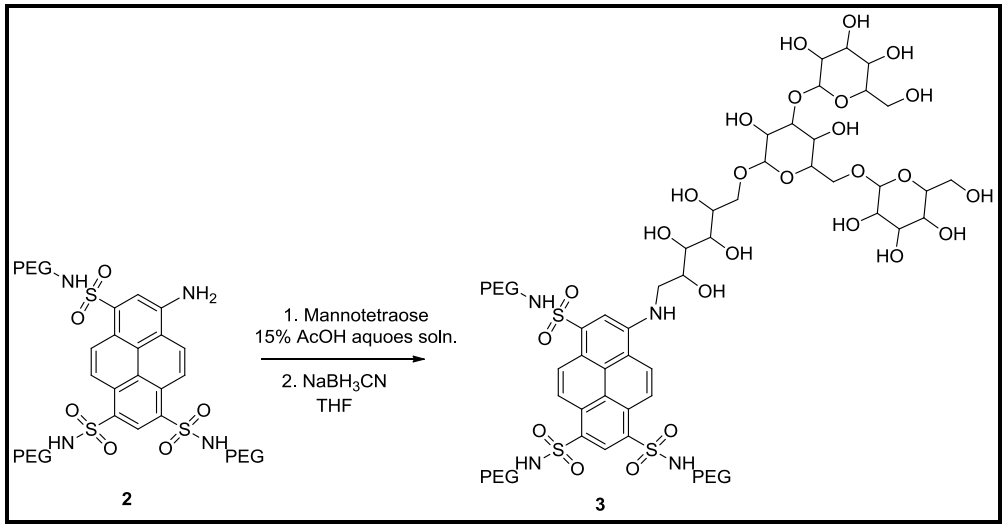

Figure 25. Synthesis of PEGylated APTS-MT via reductive amination to increase the size of the ligand with a single fluorophore and three PEG chains.

A HiTrap ConA column was then used to purify the sample after dialysis was used to remove the unbound mannotetraose. Absorbance measurements were taken to confirm presence of the conjugated sugar which was expected to result in an additional 20 nm wavelength redshift if present. It was observed from Figure 26 that the only a 4 nm wavelength shift occurred. Furthermore, this solution was not able to bind to the ConA column indicating that either the sugar was not conjugated successfully or the PEG chains were hindering binding of the sugar to ConA or the conjugation of the sugar to the dye.

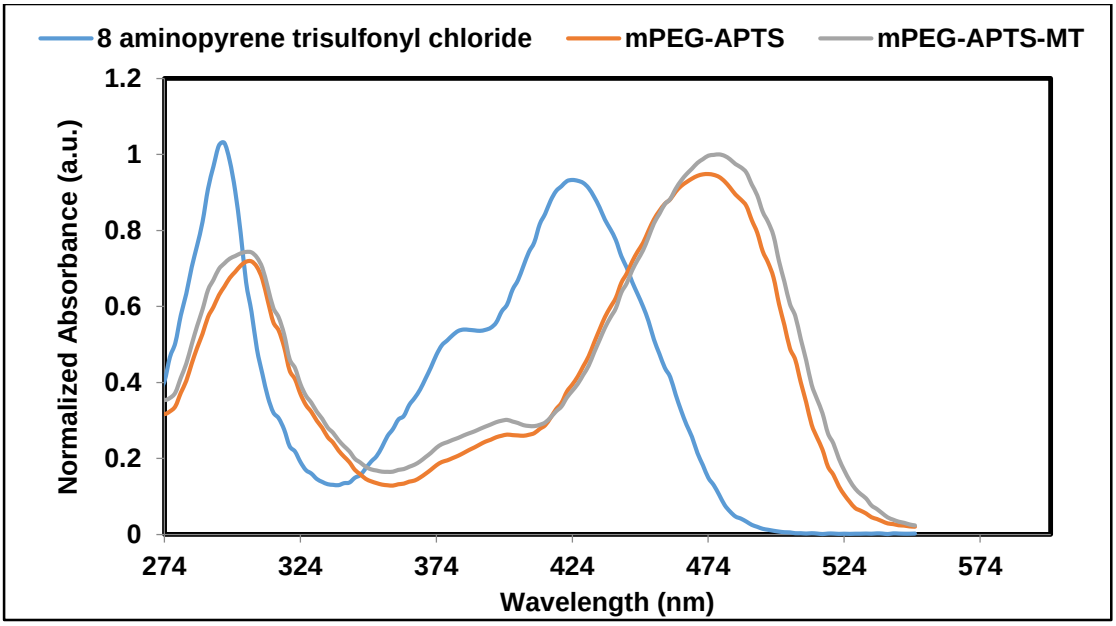

Figure 26. Absorbance spectroscopy scan after the conjugated of the competing ligand, mannotetraose, indicating no apparent shift in wavelength.

Therefore, an attempt was made to conjugate mannotetraose to the APTS dye prior to the addition of the PEG chains. A 20 nm wavelength shift was observed which indicated the presence of mannoetraose (Figure 27).

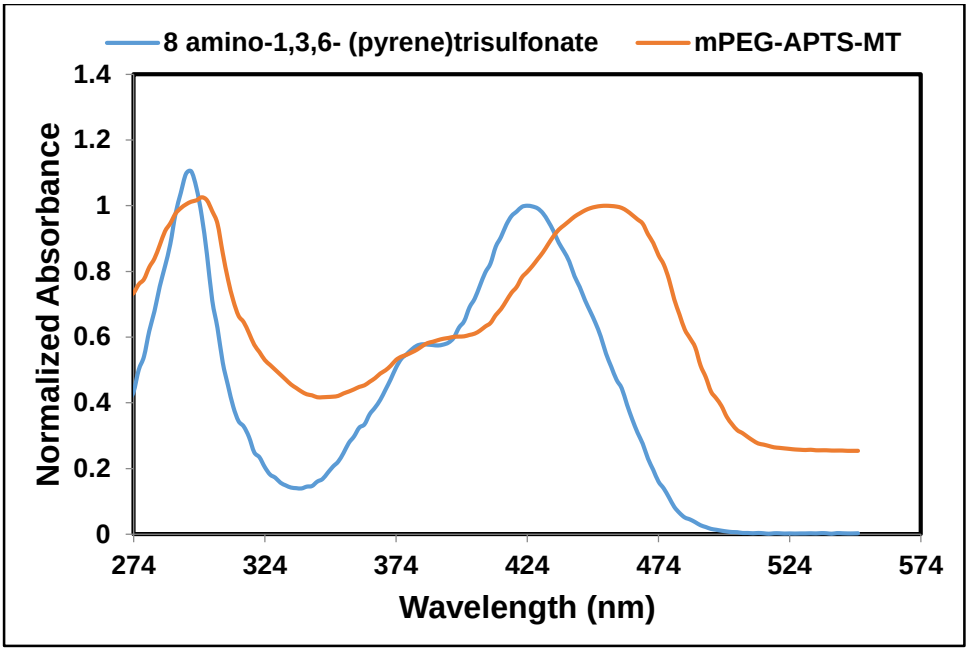

Figure 27. Absorbance spectroscopy scan after the conjugated of the competing ligand followed by the PEGylation of the fluorophore indicating a significant shift in wavelength.

Based on these results it was concluded that although PEGylation of APTS is possible the free steric hindrance of the chains did not allow for the successful conjugation of the competing ligand, mannotetraose and could potentially hinder the binding of the ligand to ConA. However, the potential to conjugate the PEG chains to the dye could play a significant role in the immobilization of APTS-MT to the walls of the AMPS-PNIPAAm rods which was investigated and described in a later section of this work.

Layer-by-Layer on PINIPAAm Inner Wall

Directly embedding the assay within the AMPS-PNIPAAm hydrogel rod is desirable because the loading efficiency of the assay can be controlled. This can be achieved by utilizing LbL, similar to the previous microencapsulation technique, where the bilayer can potentially serve as a semipermeable membrane.

The poly-electrolytes used were prepared at pH 8 in 5 mM sodium bicarbonate buffer: $PDADMAC^+$ (2 mg/mL), PSS^- (2 mg/mL), and RITC-PAH^+ (2 mg/mL). The hydrogel was then connected to inlet and outlet needles as shown in Figure 18. Next, the inner surface of the hydrogel rod synthesized above was washed by flowing 5 mL of DI H_2O through the gels three times, via a 5 mL syringe. For imaging purposes, 5 Bilayers of RITC-PAH^+/ PSS^- was deposited on the inner wall of the hydrogel rod. RITC-PAH^+ allow for the imaging of the layers via fluorescence microscopy. Briefly, 1 mL of RITC-PAH^+ was deposited first on the inner walls of the hollow rod hydrogel since its overall charge is negative. After 1 minute, 5 mL of DI H_2O was injected into the rod to wash away any residues that did not attach electrostatically to the wall. Following this wash, 1 mL of PSS^- was injected in a similar manner into the rod and after allowing it to interact with the previous layer for 1 minute the inner walls were again washed with 5 mL of DI H_2O. This was repeated until all 5 bilayers were deposited; then the rod was washed 3 times with DI H_2O. Bright-field and fluorescence images were then taken via a Nikon Eclipse TE2000-U Inverted Microscope (Nikon Instruments Inc., Melville, NY). A hydrogel without layers was also imaged under the same microscope as a control.

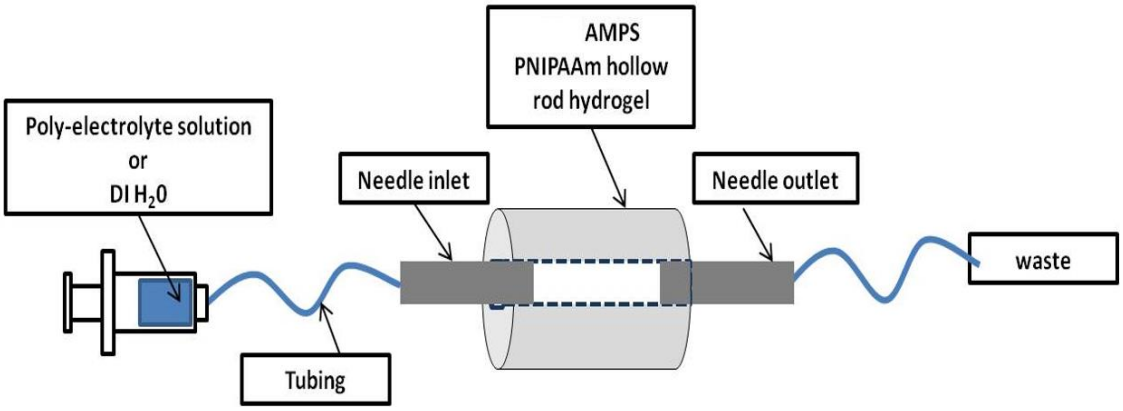

Figure 28. Schematic of LbL experimental set-up.

The fluorescence image in Figure 19 showed that the poly-electrolyte layers adhered to inner wall of the hydrogel. Furthermore, based on the absence of fluorescence within the walls of the hydrogels, we can conclude that the poly-electrolytes did not diffuse into the walls of the hydrogel rod.

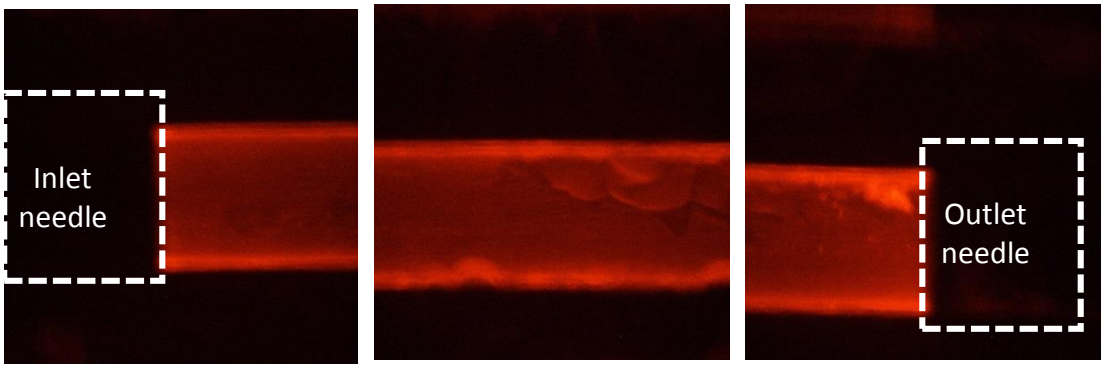

Figure 29. Fluorecence image of the LbL layers within the inner channel of the AMPS-PNIPAAm. Fluorescence is due to the Rhodamine dye conjugated to the positively charged polyelectrolyte, PAH^+.

For the purpose of glucose response hydrogels rods were prepared in a similar manner but with only six bilayers of $PDADMAC^{+}/PSS^{-}$; since a minimum of five bilayers are needed for layer stability. The assay was then encapsulated by pipetting of 1 µL of assay (10 µM mPEG-TRITC-ConA and 2 µM APTS-MT) into the rod and capping both ends with glass beads sealed with 98% PEG (mw 575). Preliminary FRET response (Figure 30) showed a FRET increased of ~49% in response to physiologically relevant glucose concentration (600 mg/dL). This is an improvement over both the calcium carbonate and the alginate based microencapsulation techniques as well as previous direct encapsulation method when there was a negative FRET response as assay leached out in the absence of the layers. However, further characterization of this method in terms of assay leaching and glucose diffusion need to be conducted in order to determine the appropriate number of bilayers needed to retain the assay without hindering glucose diffusion.

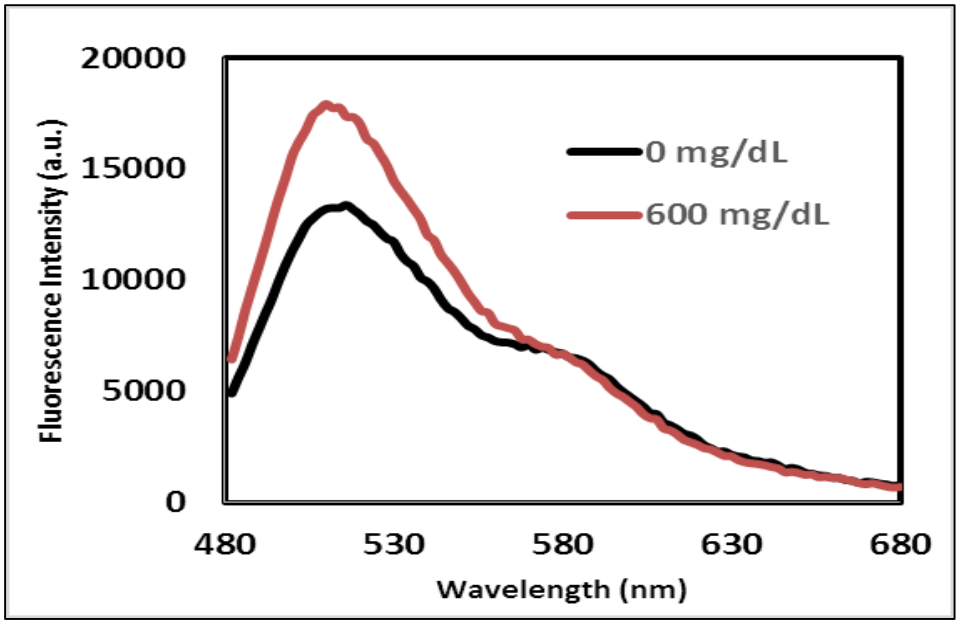

Figure 30. Glucose response of glucose biosensor after encapsulation of the assay (2 µM APTS-MT and 10 µM mPEG -TRITC-ConA) in the AMPS-PNIPAAm rods containing 6 bilayers on its inner wall.

Leaching and Glucose Diffusion Studies

From the different encapsulation and modification techniques investigated above, LbL proved to be more efficient in the ability to control concentration and loading efficiency, achieving glucose response of the encapsulated assay and in its easy fabrication. Therefore, this method was selected for further investigation in the development of the glucose biosensor.

Leaching Studies

To determine if LbL can be used to minimize leaching from the porous AMPS-PNIPAAm hydrogels, a 24 h leaching study was conducted using varying amount of

polyelectrolyte bilayers deposited on the inner walls of the hollow rod. Then the exposure of the biosensors to high concentration glucose (1000 mg/dL) allowed for the majority of the assay's components to be in their unbound state, due to the competitive binding of glucose to ConA freeing APTS-MT from its binding site. Since APTS-MT is the smaller component (~1 kDa), it would be more likely to leach out of the membrane compared to mPEG-TRITC-ConA (~104 kDa).

The supernatant data showed a decrease in APTS-MT leaching with increasing number of bilayers (Figure 31). 75-80% of APTS-MT was retaining within the membrane after at least 30 Bilayers were deposited on the inner wall of the AMPS-PNIPAAm hydrogel rods.

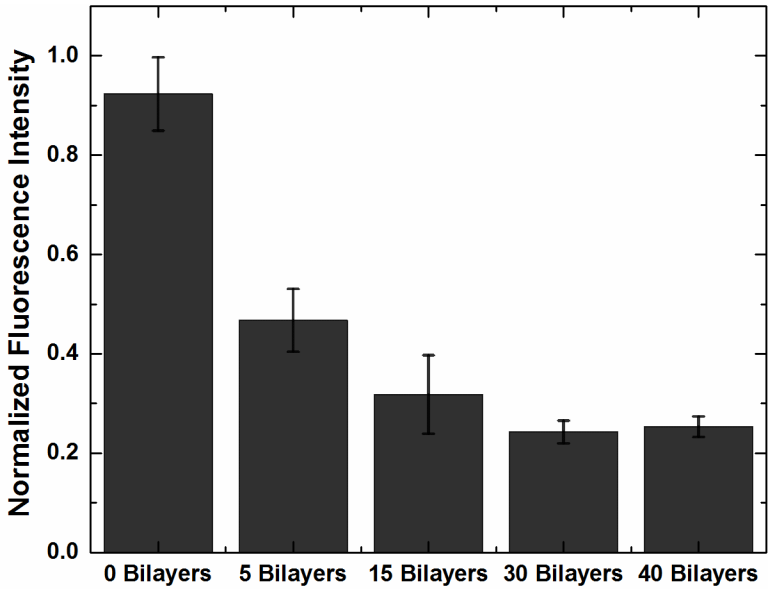

Figure 31. Fluorescence leaching study of encapsulated APTS-MT for varying bilayers of PDADMAC/PSS on the inner wall of AMPS-PNIPAAm hydrogel rods.

A more detailed leaching study comparing 0 bilayers versus 30 bilayers was conducted to show the improvement that the presence of the 30 bilayers provides. Figure 32 shows that within the first 12 h the hydrogel rods without the layers experienced a more significant leaching of APTS-MT when compared to the 30 bilayer rods.

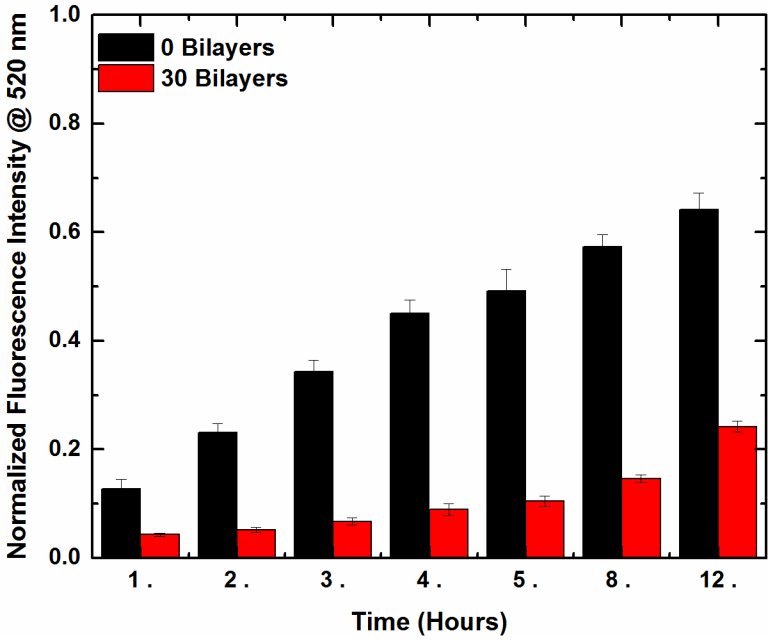

Figure 32. The average fluorescence intensity of the supernatant for three assay containing hydrogel rods exposed to high concentration glucose to compare the amount of leaching of APTS-MT from rods modified with 0 and 30 bilayers.

Although this is a significant improvement because without the layers almost all APTS-MT leached out after being displaced by a high concentration of glucose, this is still not sufficient in designing a long term implantable glucose sensor. Therefore, further modification via immobilization of APTS-MT on the inner most layer can be explored in order to try and fully retain the assay components. It should also be noted

less than 10% of the mPEG-TRITC-ConA leached out the rods regardless of the number of bilayers (Figure 33). This suggest that there is a greater need to modify the encapsulation method based on the competing ligand instead of the lectin.

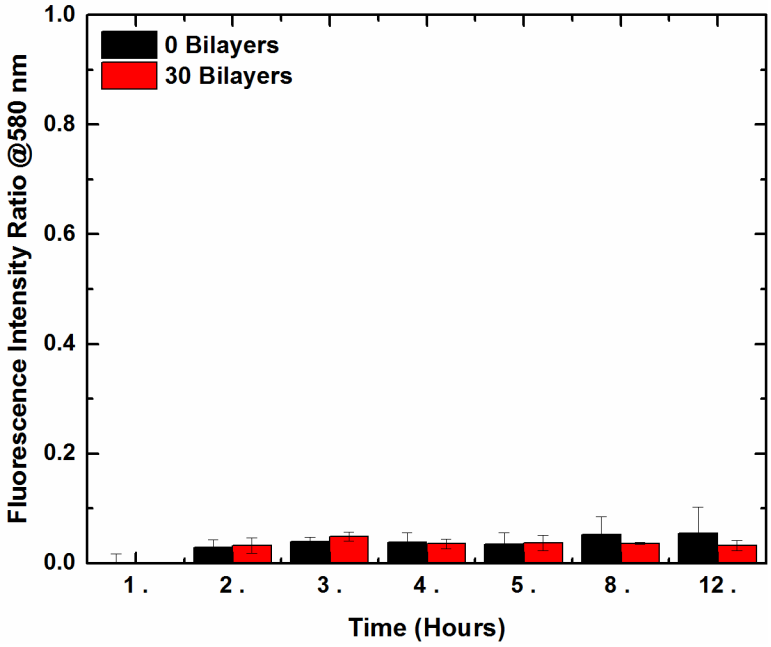

Figure 33. The average fluorescence intensity of the supernatant for three assay containing hydrogel rods exposed to high concentration glucose to compare the amount of leaching of mPEG-TRITC-ConA from rods modified with 0 and 30 bilayers.

Glucose Diffusion Studies

The purpose of these layer-by-layer (LbL) hollow rod hydrogels is to act as a biocompatible housing chamber for a glucose sensing assay and a semi-permeable membrane for glucose diffusion. Therefore, glucose diffusion studies were conducted body temperature (35 ^{o}C) on hydrogels with a range of bilayers (# of bilayers: 0, 10, 20

and 30) to determine whether the presence of the layer hindered the diffusion rate of glucose through the gel.

For this study, approximately 1.5 mm thick 25% AMPS PNIPAAm hydrogel slabs was synthesized. Using an open-face filter holder (Pall Co., Port Washington, NY), the hydrogel slab was securely clamped between the ring which allowed for only one side of the hydrogel to be exposed for LbL modification. The exposed side was washed 3 times with 10 mL DI H_2O and then the bilayers of $PDADMAC^+$/ PSS^- were deposited on its surface, in similar manner to above. The hydrogel was then removed from the filter holder and the side with the layers was marked as a means of identification in the future. The hydrogel membranes were then allowed to soak in DI H_2O for 24 hours before diffusion tests were performed.

The LbL hydrogel was then cut into smaller strips (1cm x 1cm) and placed in side-by-side diffusion chambers (PermeGear, Bethlehem, PA) with the LbL side facing the receiver chamber containing 3 mL DI H_2O. The donor chamber contained 3 mL glucose solution (~1000 mg/dL). The chambers were mounted on a stir plate set to 1000 rpm to ensure that the concentration in both chambers remained constant. The diffusion chambers were connected to a water bath pump system set to 35 ^oC.

In 20 min intervals, 50 µL of solution was extracted from each chamber via a pipette for a period of 3 hours. An YSI 2300 Stat Plus Biochemistry Analyzer (YSI Inc., Yellow Springs, OH) was then used to determine the concentration of glucose present in the extracted samples. Then the diffusion coefficient was calculated using the following derivative form of Fick's second law of diffusion (Equation 9):

$$\frac{\partial c}{\partial t} = D\ \frac{\partial^2 c}{\partial x^2}$$

Equation 9.

Where *c* is the concentration within the receiving chamber, *t* is the time, *D* is the diffusion coefficient and *x* is the diffusion distance. Under the assumption that each chamber maintained a uniformed concentration, Equation 9 was simplified to:

$$Q_t = \frac{ADC_i}{T}\ (t - \frac{T^2}{6D})$$

Equation 10.

Where Q_t is the amount of glucose transferred through the membrane at a specific time, *t*. *A* indicates the area of the hydrogel exposed to either the donor or receiver chamber and C_i is the initial stock glucose concentration within the donor channel at *t* equal zero. *T* is the thickness of the hydrogel membrane.

Table 1. Comparing the glucose diffusion coefficient for AMPS-PNIPAAm hydrogel membranes modified with different number of bilayers.

Hydrogel Composition	**Glucose Diffusion Coefficient $cm^2\ s^{-1}$**
DN PNIPAAm Nanocomposite	$1.88 \times 10^{-6} \pm 0.001$
DN 25% AMPS no layers	$2.61 \times 10^{-6} \pm 0.13$
DN 25% AMPS 10 Bilayers	$2.68 \times 10^{-6} \pm 0.41$
DN 25% AMPS 20 Bilayers	$2.20 \times 10^{-6} \pm 0.02$
DN 25% AMPS 30 Bilayers	$2.43 \times 10^{-6} \pm 0.13$

Results indicated that the presence of the layers did not significantly hinder the diffusion of glucose through the hydrogel membranes when compared with hydrogel membranes consisting of no layers.

Glucose Response

The glucose response of the assay containing AMPS-PNIPAAm rods were evaluated within physiologically relevant glucose concentration (0 to 600 mg/dL) to determine its functionality, time response, sensitivity. These hydrogels were initially evaluated at room temperature.

Time Response Study

The time response of the biosensors was evaluated using a Tecan Microplate Reader. Hydrogel rods (length: (~5 mm) modified with 30 bilayers and containing 1 µL of the glucose assay (2 µM APTS-MT and 10 µM mPEG-TRITC-ConA) were each placed within a well of a 96-well plate and submerge in 200 µL of TBS solution. An initial fluorescence scan was taken to determine the FRET signal at 0 mg/dL. Next, the concentration of the solution was increased to 600 mg/dL using a stock concentration of glucose (~50, 000 mg/dL). Fluorescence measurements (λ_{em} range: 480 nm to 680 nm) were taken every 10 minutes until the signal stabilized.

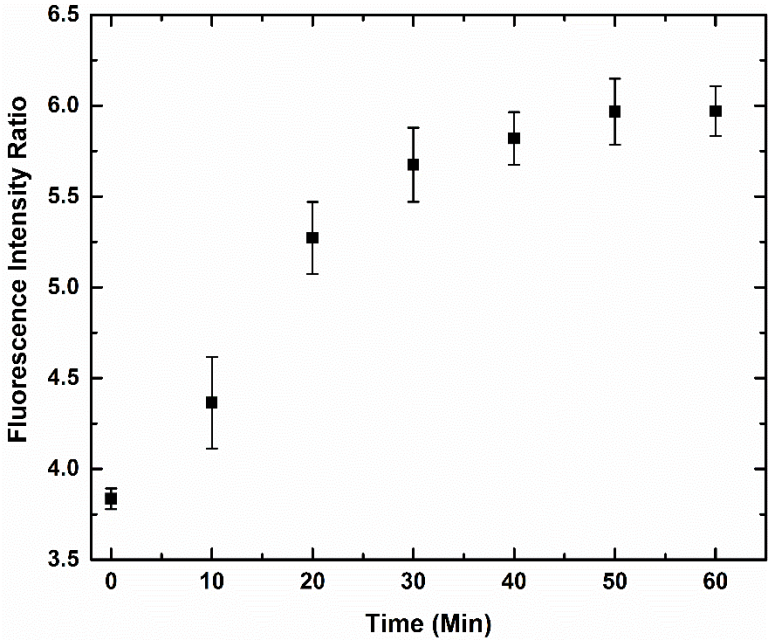

Figure 34. The average time response of three 30 bilayer AMPS-PNIPAAm hydrogel rods containing 1 µL of the glucose sensing assay (2 µM APTS-MT and 10 µM mPEG-TRITC-ConA) in the presence of 600 mg/dL glucose concentration.

Figure 34 indicated that the FRET signal reached stability after approximately 30 minutes. Ideally the time response goal is approximately 5 to 10 minutes. Based on the LbL glucose diffusion data (Table 1) the presence of the layers does not play a significant role in the sensors response time. Therefore, one potential solution to increasing the response time would be to increase the porosity of the AMPS-PNIPAAm membrane.

Glucose Response Sensitivity Study

Thus far the glucose biosensor has only been evaluated at the high concentration of the physiological relevant range. Therefore, this study aimed to investigate the sensitivity of the sensor for concentrations within this range (0 to 600 mg/dL). AMPS-PNIPAAm rods containing the assay were prepared similarly to previous method where 1 µL of the assay were encapsulated within the 30 bilayers rods. Fluorescence measurements were taken for each glucose concentration after 15 minutes wait time.

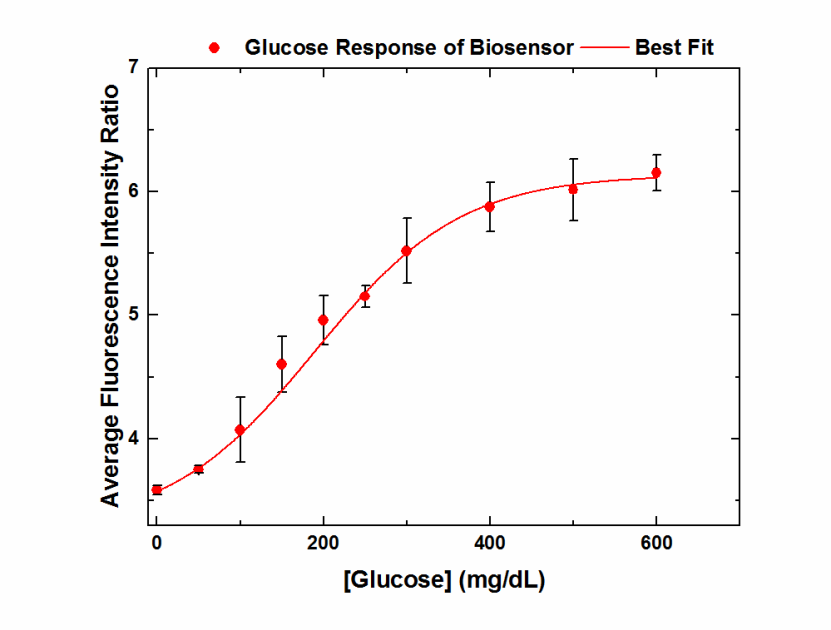

Figure 35. The average FRET response of three 30 bilayer AMPS-PNIPAAm hydrogel rods containing 1 µL of the glucose sensing assay (2 µM APTS-MT and 10 µM mPEG-TRITC-ConA) in the presence of varying concentrations of glucose (0 to 600 mg/dL) within the physiological relevant range.

Figure 35 shows that the biosensors can track changes in glucose concentrations. This data was fitted to a typical competitive binding curve and the predicted versus

actual glucose concentration plot was obtained (Figure 36). This results indicated that the assay can track changes in glucose concentration with a MARD of ~10 ± 0.9%. This MARD is comparable to the CGM devices proposed by various research groups whose *in vivo* MARD% ranged from 11% to 16%.[16-18]

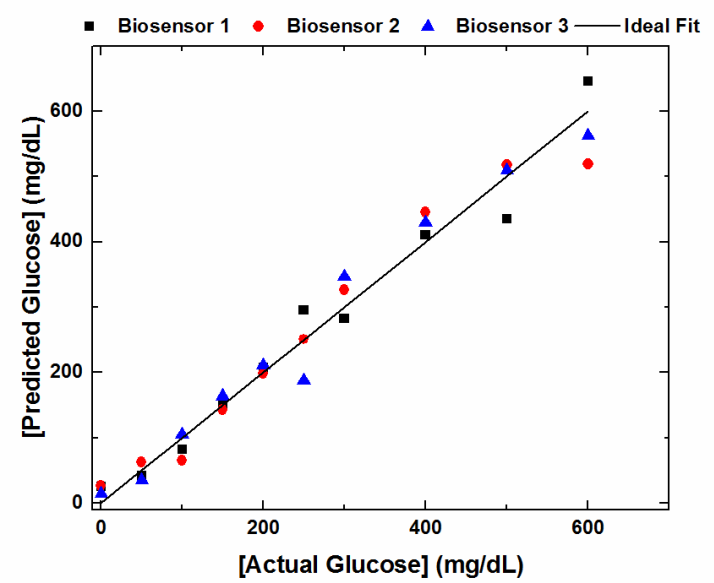

Figure 36. Preliminary result showing predicted versus actual glucose response of three 30 bilayer AMPS-PNIPAAm assay containing hydrogel rods showing ability to predict changes in glucose concentrations with a MARD around 10%.

Long Term Glucose Response Study

The lifetime of current commercially FDA approved CGM device is three to seven days. Therefore, the proposed glucose sensor within this work was evaluated to determine its response over a week. Fluorescence measurements were taken each day for seven days for glucose concentrations at 0 mg/dL (TBS only) and 600 mg/dL.

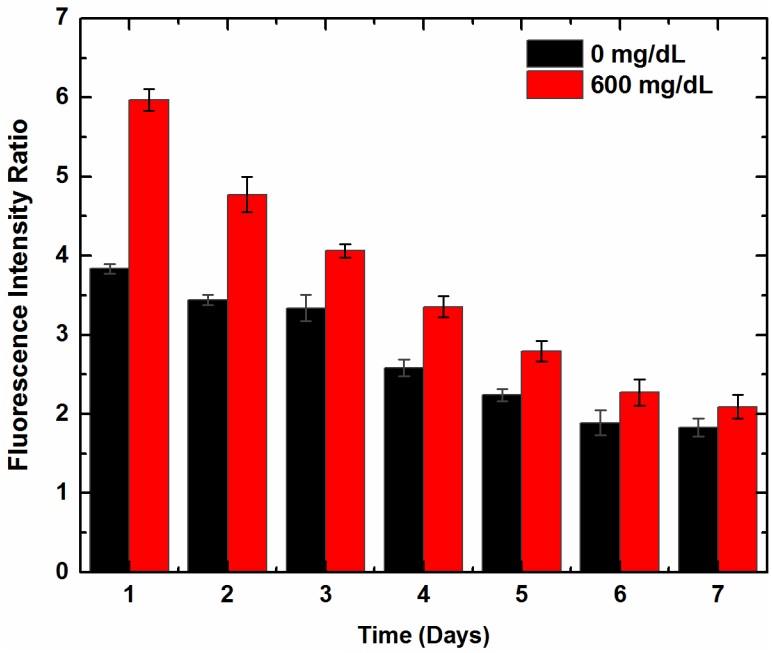

Figure 37. The average glucose response of three biosensors over seven days to determine its longevity.

Results indicated that the sensor has the ability to sense glucose up to 2 days (Figure 37). However, after the first day a decrease from 56% to 39% in the FRET signal was observed and the signal continued to decrease over the course of 7 days. This result indicates the need for further improvement on the LbL technique to improve on the retention of the assay within the AMPS-PNIPAAm hydrogel rod. This can be accomplished in two ways by either crosslinking the polyelectrolyte layers within the LbL or by immobilizing the APTS-MT on the layers.

CHAPTER V

IMMOBILIZATION OF APTS-MT ON INNER WALL OF AMPS-PNIPAAM

From the leaching studies above it was observed that only 75-80% of the assay was retained in the membrane after 24 h. This is not ideal when aiming to develop a long term implantable sensor. APTS-MT, the smaller component of the assay, had a higher percentage of leaching compared to mPEG-TRITC-ConA. Using the same LbL technique, an alternative negatively charged polyelectrolyte, poly (4-styrenesulfonic acid-co-maleic acid) sodium salt (PSS-co- maleic acid), can allow for APTS-MT to be immobilized on the layers via a PEG linker chain (NH_2-PEG_{800}-NH_2; Nanocs) and similar to the techniques used when attempting to bulk up of the molecule.

Immobilization of APTS-MT

For the LbL, 10 bilayers of PDADMAC/PSS-co-maleic aid was deposited on the inner wall of the AMPS-PNIPAAm rods. These PSS-co-maleic acid layers provide free carboxylic acid functional groups that can be used to bind amine reactive groups to it. In this work bifunctional PEG-amine (PEG MW 800 Da) was attached to these free carboxylic groups using a standard NHS/EDC reaction. Following the addition of the bifunctional PEG linker the CL dye in the form of 2-acrylamido-2-methylpropane trisulfonyl chloride was allowed to react with the free amine of the linker via the same chemical reaction used in the synthesis of bulk up APTS-MT described in Figure 23.

The presence of the immobilized dye was confirmed via Fluorescence images (Figure 37) after washing at least five times with DI H_2O and soaking in DI H_2O overnight to remove any free dye.

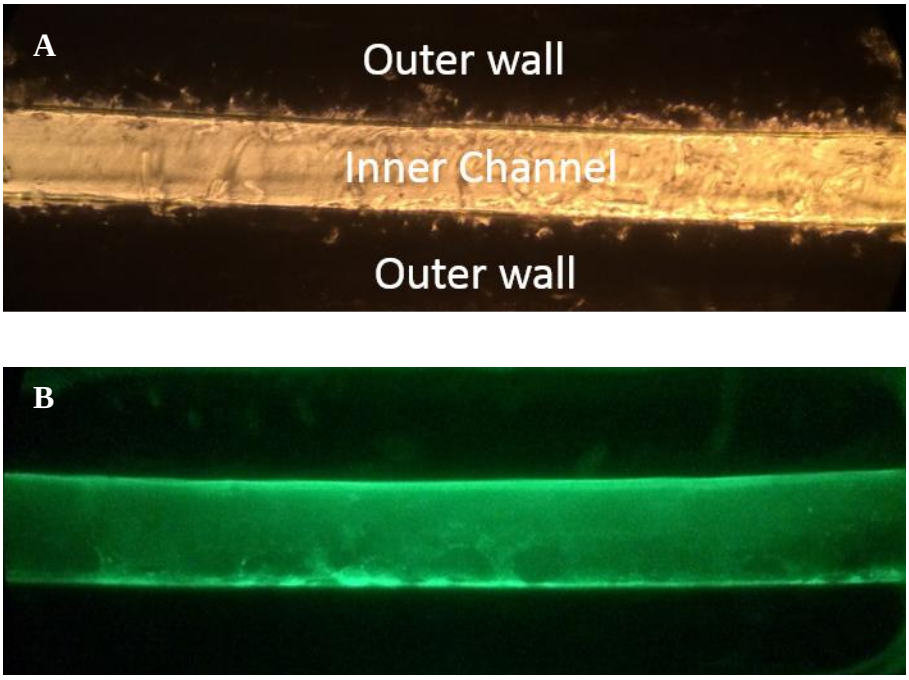

Figure 38. (A) Bright field image and (B) Fluorecence image of immobilized the donor fluorophore, APTS, via LbL layers within the inner channel of the AMPS-PNIPAAm.

An attempt was then made to conjugate mannotetraose to the immobilized dye using the Prozyme® Amine Reduction that was previously used to synthesize APTS-Dextran. The excess/unconjugated dye was removed via several DI H_2O washes and absorbance measurements were taken to determine the excitation wavelength of the immobilized molecule as a means to determine the success of the reaction. It is expected that the peak absorbance wavelength should shift from ~420 nm to ~450 nm from the conjugation of the dye alone to the dye bound to mannotetraose which was confirmed by

absorbance scan on the hydrogel rod. This method requires further optimization to obtain the desired molar concentration of APTS-MT conjugated to the LbL wall for the next generation to be able to sense changes in glucose concentrations.

CHAPTER VI

SUMMARY AND FUTURE WORK

In summary, the goal of this research was to design and encapsulate a thermally stable, non-aggregative ConA-based competitive binding assay, towards the overall goal of producing a continuous glucose monitoring biosensor.

Previous work used native unbound ConA as the glucose receptor. The assays generated with this ConA resulted in constant aggregation of ConA and inconsistency in the assay's sensitivity to glucose. Furthermore, previous assay contained the use of competing ligands such as dextran and glycosylated dendrimer. Even though these two competing ligands demonstrated response to glucose when tested with physiological relevant concentrations, the extent at which their assays fluorescence changed in response to glucose was either small or inconsistent. Therefore, there was a need to investigate an alternative assay composition to improve its sensitivity and overcome these problems. Recent work had introduced a new competing ligand, mannotetraose, as a means to improve the assay's sensitivity. Therefore, there was a need to characterize the new assay's sensitivity and stability. Also, prior to this date the functionality of this assay within the designed biocompatible membrane was not yet determined due to the need to further characterize the membrane's biocompatibility, cell toxicity and mechanical properties. Therefore, this work aimed to encapsulate and characterize the assay's functionality within this membrane.

It was determined that PEGylation of ConA would aid in the stability of the protein at body temperature minimizing the chances of the protein undergoing thermal unfolding and aggregation. This work also noted that the use of PEGylation did not hinder ConA's ability in binding to a competing ligand and its performance within a competitive binding assay to sense changes in physiologically relevant glucose concentrations. Thus generating a thermally stable glucose sensing assay.

The characterization of the competing ligand, mannotetraose, showed that this new ligand did not produce large aggregates when bound to ConA unlike the traditional ligand, dextran. Furthermore, mannotetraose proved to be more sensitive to changes in glucose concentration, over dextran, when placed within FRET based competitive binding system.

This work was the first to incorporate the assay within the biocompatible PNIPAAm based hydrogel rod and showed that the assay can still sense glucose within the physiological concentration range. A major obstacle to overcome was the size of the assay (nanoscale) versus the pore size of the hydrogel (microscale). To address this problem, various encapsulation techniques that are traditionally used to encapsulate nanoscale assays were investigated as well as the possibility of increasing the size of the smaller assay component, APTS-MT. It was determined that the best method for encapsulation would be to deposit LbL on the inner walls of the hydrogel rods and then directly inject the assay into the hollow cavity. This method allowed for the control of the loading efficiency, concentration and volume of assay used without significantly affecting the functionality of the assay. Although this technique provided improved the

retention of the assay inside the hydrogel rod, as a long term sensor there is still need for improvement as it was observed that over a week the change in FRET signal dropped due to leaching of the smaller assay component.

Future work involves the design and characterization of a second generation biosensor which contains the competing ligand immobilized on the LbL wall of the biocompatible hydrogel rods in the hopes of producing a long term glucose biosensor. This is currently being investigated in the Optical Biosensing Lab. In addition, new FRET pair fluorophores could be chosen which excites and emits further into the red wavelength range. This is needed to minimize the background noise from the tissue's optical properties.

REFERENCES

1. Center for Diease Control and Prevention. “National Diabetes Statistics Report: Estimates of Diabetes and Its Burden in the United States, 2014,” http://www.cdc.gov/diabetes/data/national.html (accessed May 14, 2016).
2. World Health Organization. “Diabetes Fact Sheet,” http://www.who.int/topics/diabetes_mellitus/en/ (accessed May 15, 2016).
3. American Diabetes Association. “Diabetes Basics,” http://www.diabetes.org/diabetes-basics/ (accessed May 15, 2016).
4. American Diabetes Association. “Economic Costs of Diabetes in the U.S. in 2012,” *Diabetes Care*, **2013**. DOI: 10.2337/dc12-2625.
5. Clarke, S.; Foster, J. “A history of blood glucose meters and their role in self-monitoring of diabetes mellitus,” *British Journal of Biomedical Science* **2012**, 69, (2), 83.
6. Jarrett, R.; Keen, H.; Hardwick, C. ““Instant” blood sugar measurement using Dextrostix and a reflectance meter,” *Diabetes* **1970,** 19, (10), 724-726.
7. Junker, K.; Ditzel, J. “Inaccuracy of Test Strips with Reflectance Meter in Determination of High Blood-Sugars,” *The Lancet* **1972**, 299, (7755), 815-817. DOI: 10.1016/S0140-6736(72)90800-8.
8. Yamada, S. “Historical Achievements of Self-Monitoring of Blood Glucose Technology Development in Japan,” *Journal of Diabetes Science and Technology* **2011**, 5, (5), 1300-1306. DOI: 10.1177/193229681100500541.

9. Enejder, A. M.; Scecina, T. G.; Oh, J.; Hunter, M.; Shih, W.; Sasic, S.; Horowitz, G. L.; Feld, M. S. “Raman spectroscopy for noninvasive glucose measurements,” *Journal of Biomedical Optics* **2005**, 10, (3), 031114-0311149. DOI: 10.1117/1.1920212.
10. Coté, G. L.; Fox, M. D.; Northrop, R. B. “Noninvasive optical polarimetric glucose sensing using a true phase measurement technique,” *Biomedical Engineering, IEEE Transactions* **1992**, 39, (7), 752-756. DOI: 10.1109/10.142650.
11. Mohammadi, L. B.; Klotzbuecher, T.; Sigloch, S.; Welzel, K.; Goeddel, M.; Pieber, T.; Schaupp, L. “Clinical performance of a low cost near infrared sensor for continuous glucose monitoring applied with subcutaneous microdialysis,” *Biomedical Microdevices* **2015**, 17, (4), 1-10. DOI: 10.1007/s10544-015-9983-4.
12. Weiss, S. “Fluorescence spectroscopy of single biomolecules,” *Science* **1999**, 283, (5408), 1676-1683. DOI: 10.1126/science.283.5408.1676.
13. Fang, H.; Kaur, G.; Wang, B. “Progress in boronic acid-based fluorescent glucose sensors,” *Journal of Fluorescence* **2004**, 14, (5), 481-489. DOI: 10.1023/B:JOFL.0000039336.51399.3b.
14. Yoon, J.; Czarnik, A. W. “Fluorescent chemosensors of carbohydrates. A means of chemically communicating the binding of polyols in water based on chelation-enhanced quenching,” *Journal of the American Chemical Society* **1992**, 114, (14), 5874-5875. DOI: 10.1021/ja00040a067.
15. Goldstein, I. J.; Hollerman, C. E.; Merrick, J. M. “Protein-carbohydrate interaction I. The interaction of polysaccharides with concanavalin A,” *Biochimica et*

Biophysica Acta (BBA) - General Subjects **1965**, 97, (1), 68-76. DOI: 10.1016/0304-4165(65)90270-9.

16. Goldstein, I. J.; Hollerman, C. E.; Smith, E. E. "Protein-Carbohydrate Interaction. II. Inhibition Studies on the Interaction of Concanavalin A with Polysaccharides*," *Biochemistry* **1965**, 4, (5), 876-883. DOI: 10.1021/bi00881a013.
17. Ballerstadt, R.; Evans, C.; McNichols, R.; Gowda, A. "Concanavalin A for in vivo glucose sensing: A biotoxicity review," *Biosensors and Bioelectronics* **2006**, 22, (2), 275-284. DOI:10.1016/j.bios.2006.01.008.
18. Schultz, J. S.; Mansouri, S.; Goldstein, I. J. "Affinity Sensor: A New Technique for Developing Implantable Sensors for Glucose and Other Metabolites," *Diabetes Care* **1982**, 5, (3), 245-253.DOI: 10.2337/diacare.5.3.245.
19. Ballerstadt, R.; Schultz, J. S. "A fluorescence affinity hollow fiber sensor for continuous transdermal glucose monitoring," *Analytical Chemistry* **2000**, 72, (17), 4185-4192. DOI: 10.1021/ac000215r.
20. Ballerstadt, R.; Evans, C.; Gowda, A.; McNichols, R. "In vivo performance evaluation of a transdermal near-infrared fluorescence resonance energy transfer affinity sensor for continuous glucose monitoring," *Diabetes Technology and Therapeutics* **2006**, 8, (3), 296-311. DOI: 10.1089/dia.2006.8.296.
21. Müller, A. J.; Knuth, M.; Nikolaus, K. S.; Krivánek, R.; Küster, F.; Hasslacher, C. "First Clinical Evaluation of a New Percutaneous Optical Fiber Glucose Sensor for Continuous Glucose Monitoring in Diabetes," *Journal of Diabetes Science and Technology* **2013**, 7, (1), 13-23. DOI: 10.1177/193229681300700103.

22. Nielsen, J. K.; Christiansen, J. S.; Kristensen, J. S.; Toft, H. O.; Hansen, L. L.; Aasmul, S.; Gregorius, K. “Clinical Evaluation of a Transcutaneous Interrogated Fluorescence Lifetime-Based Microsensor for Continuous Glucose Reading,” *Journal of Diabetes Science and Technology (Online)* **2009**, 3, (1), 98-109. DOI: 10.1177/193229680900300111.

23. Tang, B.; Cao, L.; Xu, K.; Zhuo, L.; Ge, J.; Li, Q.; Yu, L. “A New Nanobiosensor for Glucose with High Sensitivity and Selectivity in Serum Based on Fluorescence Resonance Enerfy Transfer (FRET) between CdTe Quantum Dots and Au Nanoparticles,” *Chemistry* **2008**, 14, (12), 3637-44. DOI: 10.1002/chem.200701871.

24. Ibey, B. L.; Beier, H. T.; Rounds, R. M.; Coté, G. L.; Yadavalli, V. K.; Pishko, M. V. “Competitive Binding Assay for Glucose Based on Glycodendrimer−Fluorophore Conjugates,” *Analytical Chemistry* **2005**, 77, (21), 7039-7046. DOI: 10.1021/ac0507901.

25. Cummins, B. M.; Garza, J. T.; Coté, G. L. “Optimization of a concanavalin A-based glucose sensor using fluorescence anisotropy,” *Analytical Chemistry* **2013**, 85, (11), 5397-5404. DOI: 10.1021/ac303689j.

26. Cummins, B. M.; Garza, J. T.; Coté, G. L. “ Limitations of current fluorescent glucose sensing assays based on competitive binding,” *International Society for Optics and Photonics BiOS* **2013**, 8591, 859103-6. DOI: 10.1117/12.2004564.

27. Cummins, B. M.; Li, M.; Locke, A. K.; Birch, D. J. S.; Vigh, G.; Coté, G. L. "Overcoming the aggregation problem: A new type of fluorescent ligand for ConA-based glucose sensing," *Biosensors and Bioelectronics* **2014**, (0).
28. Cummins, B. M.; Li, M.; Locke, A. K.; Birch, D. J.; Vigh, G.; Coté, G. L. "Overcoming the aggregation problem: A new type of fluorescent ligand for ConA-based glucose sensing," *Biosensors and Bioelectronics* **2015**, 63, 53-60. DOI: 10.1016/j.bios.2014.07.015.
29. Hardman, K. D.; Ainsworth, C. F. "Structure of concanavalin A at 2.4-Ang resolution," *Biochemistry* **1972**, 11, (26), 4910-4919. DOI: 10.1021/bi00776a006.
30. Hardman, K. D.; Ainsworth, C. F. "Binding of nonpolar molecules by crystalline concanavalin A," *Biochemistry* **1973**, 12, (22), 4442-4448. DOI: 10.1021/bi00746a022.
31. Mandai, D. K.; Brewer, C. F. "Differences in the binding affinities of dimeric concanavalin A (including acetyl and succinyl derivatives) and tetrameric concanavalin A with large oligomannose-type glycopeptides," *Biochemistry* **1993**, 32, (19), 5116-5120. DOI: 10.1021/bi00070a020.
32. Schultz, J. S.; Sims, G. "Affinity sensors for individual metabolites," *Biotechnology Bioengineering Symposium* **1979**, (9), 65-71.
33. Aloraefy, M.; Pfefer, J.; Ramella-Roman, J.; Sapsford, K. "Development and testing of a fluorescence biosensor for glucose sensing," *International Society for Optics and Photonics: Defense, Security and Sensing* **2012**, 8367, 83670H-1. DOI: 10.1117/12.920699.

34. Ballerstadt, R.; Polak, A.; Beuhler, A.; Frye, J. “In vitro long-term performance study of a near-infrared fluorescence affinity sensor for glucose monitoring,” *Biosensors and Bioelectronics* **2004**, 19, (8), 905-914. DOI: 10.1016/j.bios.2003.08.019.
35. Meadows, D.; Schultz, J. S. “Fiber-optic biosensors based on fluorescence energy transfer,” *Talanta* **1988**, 35, (2), 145-150. DOI: 10.1016/0039-9140(88)80053-5.
36. Meadows, D. L.; Schultz, J. S. “Design, manufacture and characterization of an optical fiber glucose affinity sensor based on an homogeneous fluorescence energy transfer assay system,” *Analytica Chimica Acta* **1993**, 280, (1), 21-30. DOI: 10.1016/0003-2670(93)80236-E.
37. Peng, J.; Wang, Y.; Wang, J.; Zhou, X.; Liu, Z. “A new biosensor for glucose determination in serum based on up-converting fluorescence resonance energy transfer,” *Biosensors and Bioelectronics* **2011**, 28, (1), 414-420. DOI: 10.1016/j.bios.2011.07.057.
38. Pickup, J. C.; Hussain, F.; Evans, N. D.; Sachedina, N. “In vivo glucose monitoring: the clinical reality and the promise” *Biosensors and Bioelectronics* **2005**, 20, (10), 1897-1902. DOI: 10.1016/j.bios.2004.08.016
39. Srinivasan, K. R.; Mansouri, S.; Schultz, J. S. “Coupling of concanavalin A to cellulose hollow fibers for use in glucose affinity sensor,” *Biotechnology and Bioengineering* **1986**, 28, (2), 233-239. DOI: 10.1002/bit.260280213.
40. McCartney, L. J.; Pickup, J. C.; Rolinski, O. J.; Birch, D. J. S. “Near-Infrared Fluorescence Lifetime Assay for Serum Glucose Based on Allophycocyanin-

Labeled Concanavalin A," *Analytical Biochemistry* **2001**, 292, (2), 216-221. DOI: 10.1006/abio.2001.5060.

41. Tolosa, L.; Malak, H.; Raob, G.; Lakowicz, J. R. "Optical assay for glucose based on the luminescnence decay time of the long wavelength dye Cy5™," *Sensors and Actuators B: Chemical* **1997**, 45, (2), 93-99. DOI: 10.1016/S0925-4005(97)00275-X.
42. Huet, C.; Lonchampt, M.; Huet, M.; Bernadac, A. "Temperature effects on the concanavalin A molecule and on concanavalin A binding," *Biochimica et Biophysica Acta (BBA) - Protein Structure* **1974**, 365, (1), 28-39. DOI: 10.1016/0005-2795(74)90247-5.
43. Wang, W. "Instability, stabilization, and formulation of liquid protein pharmaceuticals," *International Journal of Pharmaceutics* **1999**, 185, (2), 129-188. DOI: 10.1016/S0378-5173(99)00152-0.
44. McKenzie, G. H.; Sawyer, W. H.; Nichol, L. W. "The molecular weight and stability of concanavalin A," *Biochimica et Biophysica Acta (BBA) - Protein Structure* **1972**, 263, (2), 283-293. DOI: 10.1016/0005-2795(72)90081-5.
45. Vetri, V.; Canale, C.; Relini, A.; Librizzi, F.; Militello, V.; Gliozzi, A.; Leone, M. "Amyloid fibrils formation and amorphous aggregation in concanavalin A," *Biophysical Chemistry* **2007**, 125, (1), 184-190. DOI: 10.1016/j.bpc.2006.07.012.
46. Entlicher, G.; Koštíř, J. V.; Kocourek, J. "Studies on phytohemagglutinins. VIII. Isoelectric point and multiplicity of purified concanavalin A," *Biochimica et*

Biophysica Acta (BBA) - Protein Structure **1971**, 236, (3), 795-797. DOI: 10.1016/0005-2795(71)90266-2.

47. Stein, E. W.; Volodkin, D. V.; McShane, M. J.; Sukhorukov, G. B. "Real-Time Assessment of Spatial and Temporal Coupled Catalysis within Polyelectrolyte Microcapsules Containing Coimmobilized Glucose Oxidase and Peroxidase," *Biomacromolecules* **2006**, 7, (3), 710-719. DOI: 10.1021/bm050304j.
48. Damiano, E. R.; El-Khatib, F. H.; Zheng, H.; Nathan, D. M.; Russell, S. J. "A Comparative Effectiveness Analysis of Three Continuous Glucose Monitors," *Diabetes Care* **2012**. DOI: 10.2337/dc12-0070.
49. Roberts, M. J.; Bentley, M. D.; Harris, J. M. "Chemistry for peptide and protein PEGylation," *Advanced Drug Delivery Reviews* **2002**, 54, (4), 459-476. DOI: 10.1016/j.addr.2012.09.025.
50. Veronese, F. M.; Pasut, G. "PEGylation, successful approach to drug delivery," *Drug Discovery Today* **2005**, 10, (21), 1451-1458. DOI: 10.1016/S1359-6446(05)03575-0.
51. Bhat, R.; Timasheff, S. N. "Steric exclusion is the principal source of the preferential hydration of proteins in the presence of polyethylene glycols," *Protein Science* **1992**, 1, (9), 1133-1143. DOI: 10.1002/pro.5560010907.
52. Sharma, S.; Popat, K. C.; Desai, T. A. "Controlling Nonspecific Protein Interactions in Silicon Biomicrosystems with Nanostructured Poly(ethylene glycol) Films," *Langmuir* **2002**, 18, (23), 8728-8731. DOI: 10.1021/la026097f.

53. Veronese, F. M.; Mero, A.; Pasut, G. “Protein PEGylation, basic science and biological applications,” *PEGylated Protein Drugs: Basic Science and Clinical Applications*. Birkhäuser Basel **2009**, 11-31.

54. Rajan, R. S.; Li, T.; Aras, M.; Sloey, C.; Sutherland, W.; Arai, H.; Briddell, R.; Kinstler, O.; Lueras, A. M. K.; Zhang, Y.; Yeghnazar, H.; Treuheit, M.; Brems, D. N. “Modulation of protein aggregation by polyethylene glycol conjugation: GCSF as a case study,” *Protein Science* **2006**, 15, (5), 1063-1075. DOI: 10.1110/ps.052004006.

55. Rodríguez-Martínez, J. A.; Solá, R. J.; Castillo, B.; Cintrón-Colón, H. R.; Rivera-Rivera, I.; Barletta, G.; Griebenow, K. “Stabilization of α-chymotrypsin upon PEGylation correlates with reduced structural dynamics,” *Biotechnology and Bioengineering* **2008**, 101, (6), 1142-1149. DOI: 10.1002/bit.22014.

56. Wu, S.-C.; Lin, K.-L.; Wang, T.-P.; Tzou, S.-C.; Singh, G.; Chen, M.-H.; Cheng, T.-L.; Chen, C.-Y.; Liu, G.-C.; Lee, T.-W.; Hu, S.-H.; Wang, Y.-M. “Imaging specificity of MR-optical imaging agents following the masking of surface charge by poly(ethylene glycol),” *Biomaterials* **2013**, 34, (16), 4118-4127. DOI: 10.1016/j.biomaterials.2013.02.025.

57. Kim, J. J.; Park, K. “Modulated insulin delivery from glucose-sensitive hydrogel dosage forms,” *Journal of Controlled Release* **2001**, 77, (1–2), 39-47. DOI: 10.1016/S0168-3659(01)00447-3.

58. Kim, J. J.; Park, K. “Glucose-binding property of pegylated concanavalin A,” *Pharmaceutical Research* **2001**, 18, (6), 794-799. DOI: 10.1023/A:1011084312134.

59. Agrawal, B. B. L.; Goldstein, I. J. “Protein-Carbohydrate interaction: VII. Physical and chemical studies on concanavalin A, the hemagglutinin of the jack bean,” *Archives of Biochemistry and Biophysics* **1968**, 124, (0), 218-229. DOI: 10.1016/0003-9861(68)90322-6.

60. Stocks, S. J.; Jones, A. J. M.; Ramey, C. W.; Brooks, D. E. “A fluorometric assay of the degree of modification of protein primary amines with polyethylene glycol,” *Analytical Biochemistry* **1986**, 154, (1), 232-234. DOI: 10.1016/0003-2697(86)90520-8.

61. Wen, Z.; Niemeyer, B. “Preparation and characterization of PEGyated Concanavalin A for affinity chromatography with improved stability,” *Journal of Chromatography B* **2011**, 879, (20), 1732-1740. DOI: 10.1016/j.jchromb.2011.04.018.

62. Hardman, K. D.; Wood, M. K.; Schiffer, M.; Edmundson, A. B.; Ainsworth, C. F. “Structure of concanavalin A at 4.25-ångström resolution,” *Proceedings of the National Academy of Sciences of the United States of America* **1971**, 68, (7), 1393-1397.

63. Jameson, D. M.; Ross, J. A. “Fluorescence Polarization/Anisotropy in Diagnostics and Imaging,” *American Chemical Society: Chemical Reviews* **2010**, 110, (5), 2685-2708. DOI: 10.1021/cr900267p.

64. Jameson, D. M.; Sawyer, W. H. “Fluorescence Anisotropy Applied to Biomolecular Interactions,” *Methods in Enzymology: Biochemical Spectroscopy* **1995**, 246, 283-300. DOI: 10.1016/0076-6879(95)46014-4.

65. Park, J. M.; Muhoberac, B. B.; Dubin, P. L.; Xia, J. “Effects of protein charge heterogeneity in protein-polyelectrolyte complexation,” *Macromolecules* **1992**, 25, (1), 290-295. DOI: 10.1021/ma00027a047.

66. Clegg, R. “The History of FRET,” *Reviews in Fluorescence 2006 Springer US* **2006**, (2006), 1-45. DOI: 10.1007/0-387-33016-X_1.

67. Albalasmeh, A. A.; Berhe, A. A.; Ghezzehei, T. A. “A new method for rapid determination of carbohydrate and total carbon concentrations using UV spectrophotometry,” *Carbohydrate Polymers* **2013**, 97, (2), 253-261. DOI: 10.1016/j.carbpol.2013.04.072.

68. Benzeval, I. D. “Development of responsive polymers for drug delivery applications,” *PhD. Dissertation, University Library* **2009**.

69. Wu, P.; Brand, L. “Resonance energy transfer: methods and applications,” *Analytical Biochemistry* **1994**, 218, (1), 1-13. DOI: 10.1006/abio.1994.1134.

70. Chinnayelka, S.; Zhu, H.; McShane, M. “Near-Infrared Resonance Energy Transfer Glucose Biosensors in Hybrid Microcapsule Carriers,” *Journal of Sensors* **2008**, 2008, 11. DOI: 10.1155/2008/346016.

71. Hou, Y.; Matthews, A. R.; Smitherman, A. M.; Bulick, A. S.; Hahn, M. S.; Hou, H.; Han, A.; Grunlan, M. A. “Thermoresponsive nanocomposite hydrogels with cell-releasing behavior,” *Biomaterials* **2008**, 29, (22), 3175-3184. DOI: 10.1016/j.biomaterials.2008.04.024.

72. Fei, R.; George, J. T.; Park, J.; Grunlan, M. A. “Thermoresponsive nanocomposite double network hydrogels,” *Soft Matter* **2012**, 8, (2), 481-487. DOI: 10.1039/C1SM06105D.

73. Abraham, A. A.; Fei, R.; Coté, G. L.; Grunlan, M. A. “Self-Cleaning Membrane to Extend the Lifetime of an Implanted Glucose Biosensor,” *American Chemical Society: Applied Materials and Interfaces* **2013**, 5, (24), 12832-12838. DOI: 10.1021/am4040653.

74. Gant, R.; Abraham, A.; Hou, Y.; Cummins, B.; Grunlan, M.; Coté, G. “Design of a self-cleaning thermoresponsive nanocomposite hydrogel membrane for implantable biosensors,” *Acta Biomaterialia* **2010**, 6, (8), 2903-2910. DOI: 10.1016/j.actbio.2010.01.039.

75. Khalil, E.; Kretsos, K.; Kasting, G. B. “Glucose Partition Coefficient and Diffusivity in the Lower Skin Layers,” *Pharmaceutical Research* **2006**, 23, (6), 1227-1234. DOI: 10.1007/s11095-006-0141-9.

76. Fei, R.; George, J. T.; Park, J.; Means, A. K.; Grunlan, M. A. “Ultra-strong thermoresponsive double network hydrogels,” *Soft Matter* **2013**, 9, (10), 2912-2919. DOI: 10.1039/C3SM27226E.

77. Fei, R.; Means, A. K.; Abraham, A. A.; Locke, A. K.; Coté, G. L.; Grunlan, M. A. “Self-Cleaning, Thermoresponsive P (NIPAAm-co-AMPS) Double Network Membranes for Implanted Glucose Biosensors,” *Macromolecular Materials and Engineering* **2016**. DOI: 10.1002/mame.201600044.

78. Fujiwara, M.; Shiokawa, K.; Morigaki, K.; Zhu, Y.; Nakahara, Y. “Calcium carbonate microcapsules encapsulating biomacromolecules,” *Chemical Engineering Journal* **2008**, 137, (1), 14-22. DOI: 10.1016/j.cej.2007.09.010.

79. Volodkin, D. V.; Larionova, N. I.; Sukhorukov, G. B. “Protein Encapsulation via Porous CaCO3 Microparticles Templating,” *Biomacromolecules* **2004**, 5, (5), 1962-1972. DOI: 10.1021/bm049669e.

80. Petrov, A. I.; Volodkin, D. V.; Sukhorukov, G. B. “Protein—calcium carbonate coprecipitation: a tool for protein encapsulation,” *Biotechnology Progress* **2005**, 21, (3), 918-925. DOI: 10.1021/bp0495825.

81. Nagaraja, A. T.; Pradhan, S.; McShane, M. J. “Poly (vinylsulfonic acid) assisted synthesis of aqueous solution stable vaterite calcium carbonate nanoparticles,” *Journal of Colloid and Interface Science* **2014**, 418, 366-372. DOI: 10.1016/j.jcis.2013.12.008.

82. Locke, A. K.; Cummins, B. M.; Abraham, A. A.; Coté, G. L. “PEGylation of Concanavalin A to improve its stability for an in vivo glucose sensing assay,” *Analytical Chemistry* **2014**, 86, (18), 9091-9097. DOI: 10.1021/ac501791u.

83. Russell, R.; Pishko, M.; Gefrides, C.; Cote, G. “A fluorescent glucose assay using poly-L-lysine and calcium alginate microencapsulated TRITC-succinyl-concanavalin A and FITC-dextran,*” Proceedings of the 20th Annual International Conference of the IEEE* **1998**, 6, 2858-2861. DOI: 10.1109/IEMBS.1998.746080.

84. Swati, M.; Srivastava, R. “Polyelectrolyte-coated alginate microspheres for optical urea sensing,” *9th IEEE Nanotechnology Conference* **2009**, 846-849.